



ELSEVIER

Precambrian Research 116 (2002) 237–263

**Precambrian
Research**

www.elsevier.com/locate/precamres

U–Pb geochronology from Tonagh Island, East Antarctica: implications for the timing of ultra-high temperature metamorphism of the Napier Complex

C.J. Carson ^{a,*}, J.J. Ague ^a, C.D. Coath ^b

^a *Department of Geology and Geophysics, Yale University, P.O. Box 208109, New Haven, CT 06520-8109, USA*

^b *Department of Earth and Space Science, University of California, Los Angeles, CA 90095-1567, USA*

Accepted 13 February 2002

Abstract

Ion microprobe U–Pb zircon geochronology of an orthopyroxene-bearing felsic orthogneiss from central Tonagh Island, Enderby Land, East Antarctica provides insight into the chronological-metamorphic evolution of the Archaean Napier Complex, the details of which have been the source of debate for over two decades. The orthogneiss crystallised at 2626 ± 28 Ma, predating peak, ultra-high temperature (UHT) metamorphism and development of an intense regional S_1 gneissosity. Two subsequent episodes of zircon growth/resetting can be identified. A minor period of zircon growth occurred at 2546 ± 13 Ma, the regional significance and geological nature of which is unclear. This was followed by an episode of abundant zircon growth, as mantles on ~ 2626 Ma cores and as anhedral grains, partly characterised by high Th/U (> 1.2), at ~ 2450 – 2480 Ma. This age coincides with both lower and upper concordia intercept ages from other U–Pb zircon studies, and several Rb–Sr and Sm–Nd whole-rock isochron ages from the Napier Complex. We conclude that UHT metamorphism occurred at ~ 2450 – 2480 Ma, and find no compelling evidence that UHT occurred much earlier as has been postulated. The zircon U–Pb data from this study also indicates a lower intercept age of ~ 500 Ma, which coincides with the emplacement of Early Palaeozoic pegmatite swarms and synchronous infiltration of aqueous fluids into the southwestern regions of the Napier Complex. © 2002 Elsevier Science B.V. All rights reserved.

Keywords: Napier Complex; East Antarctica; U–Pb geochronology; Zircon; Ion probe

1. Introduction

The granulite-facies Archaean Napier Complex of Enderby Land, East Antarctica has received

considerable attention over the past four decades (e.g. Sheraton et al., 1987; Harley and Black, 1987, 1997), initially by Soviet and Australian geological expeditions, and, in recent years, by Japanese expeditions. The identification of unusual metamorphic mineral assemblages on a regional scale, such as sapphirine + quartz (Dallwitz, 1968), osumilite \pm garnet, and orthopy-

* Corresponding author. Present address: Geological Survey of Canada, 601 Booth Street, Ottawa, Ont., Canada K1A 0E8.
E-mail address: chris.carson@nrcan.gc.ca (C.J. Carson).

roxene + sillimanite + quartz, indicative of ultra-high temperature (UHT) metamorphism, generated great interest in the geological community. Subsequent detailed petrological studies confirmed that the terrane experienced extreme temperatures approaching, even surpassing, 1000 °C at pressures of 8–11 kbars, temperatures quite unusual for mid-crustal metamorphism (Ellis, 1980; Ellis et al., 1980; Grew, 1980, 1982; Harley, 1985a, 1987, 1998; Sandiford and Powell, 1986a; Harley and Hensen, 1990; Harley and Motoyoshi, 2000). These stimulating discoveries in the petrological arena were matched by chronological reports that suggested southwestern regions of the terrane were composed of extremely ancient crustal material (Pb–Pb ages ≥ 4000 Ma; Sobotovich et al., 1976; Lovering, 1979). Although, subsequent isotopic work questioned the veracity of these very old protolith ages, an early to mid Archaean origin for many of the orthogneiss units and paragneiss sequences across the Napier Complex is now nevertheless well established (Black and James, 1983; Black et al., 1983b, 1986a,b; DePaolo et al., 1982; Owada et al., 1994; Harley and Black, 1997). However, the temporal framework of the structural-metamorphic evolution of the Napier Complex, in particular the timing of UHT metamorphism, remains a source of some debate amongst researchers (DePaolo et al., 1982; Harley and Black, 1997; Grew, 1998). In this paper, we present new zircon U–Pb ion probe data from Tonagh Island, Amundsen Bay, in which we offer additional evidence and constraints concerning the timing of UHT tectonothermal events within the Napier Complex.

2. Geological setting

The Archaean Napier Complex is located within the East Antarctic Shield between latitudes 66°–68°S and longitudes 48°–57°E and occupies much of Enderby Land (Fig. 1). The south-western regions of the Complex, well exposed as near-shore islands and coastal mountains in the vicinity of Amundsen and Casey Bays, also include several broadly east–west trending ranges of nunataks and massifs of the Tula, Scott and Raggatt

Mountains. Inland, to the north and east of Amundsen Bay, lie the scattered and sparsely exposed nunataks of the Napier Mountains. Although the precise location of the boundary is uncertain (Fig. 1), to the south and southeast the Napier Complex is juxtaposed against the granulite-facies early Neoproterozoic Rayner Complex (~ 1000 Ma; e.g. Black et al., 1987; Harley and Hensen, 1990; Kelly et al., 2000). The south-western Napier Complex is now thought to be bound by Rayner Complex material, reworked by the eastward extension of Early Palaeozoic Lützow–Holm Complex tectonism (520–550 Ma; Shirashi et al., 1997).

The geological evolution of the Napier Complex presented here is condensed from Sheraton et al. (1987) and Harley and Black (1987) and represents the generally accepted framework for the terrane. The Complex is dominated by tonalitic to granitic orthogneisses, with locally extensive layered paragneiss sequences, which include quartzites, ironstones, aluminous meta-pelites and -psammites. Mafic and ultramafic units are present, usually as narrow layers and boudinaged pods within felsic gneisses and layered paragneiss sequences. Calc-silicates and anorthosite bodies are rare. The first recognised deformation, D_1 , resulted in the development of a regional intense, flat-lying, strongly-lineated S_1 gneissosity and the transposition and interleaving of lithological units. The second deformation, D_2 , resulted in refolding of S_1 about F_2 tight asymmetrical folds with recumbent to reclined axial planes but only localised S_2 development. The third deformation, D_3 , resulted in upright broad (1–10 km) folding and produced regional dome and basin structures. In the Field Islands (Fig. 1), D_3 was sufficiently intense to have developed a penetrative fabric, but over much of the Napier Complex S_3 development was not pervasive and only locally developed in F_3 hinges. UHT metamorphic conditions are thought to have evolved during D_1 – D_2 with upper-amphibolite conditions prevailing during D_3 , after which the Complex was essentially cratonised. Petrological studies have demonstrated that the P–T evolution of the Napier Complex followed a near-isobaric cooling trajectory follow-

ing peak UHT conditions (Harley and Hensen, 1990). Tholeiitic dyke swarms were emplaced at ~ 2350 and ~ 1190 Ma (Sheraton and Black, 1981), preceding the development of various localised amphibolite-facies shear zones and pseudotachylites (D_4 – D_5 ; Harley, 1985b; Sandiford, 1985), movement along which is thought to have resulted in partial exhumation of the terrane. Features associated with D_4 – D_5 have been generally attributed to the local manifestation of granulite-facies tectonism which developed in the adjacent Neoproterozoic Rayner Complex (~ 1000 Ma), though this is largely based on indirect isotopic evidence, such as imprecise U–Pb lower concordia intercepts. The precise timing of these

shear zones and pseudotachylites remain somewhat speculative. The final rock-forming events occurred with the emplacement of Early Palaeozoic planar pegmatites (500–522 Ma; Grew and Manton, 1979; Black et al., 1983a; Carson et al., 2002) and rare mafic alkaline dykes (466–482 Ma; Black and James, 1983; Miyamoto et al., 2000).

2.1. Previous geochronology

A considerable amount of geochronological information has been obtained from the Napier Complex. Initial work focused on the identification of very old crustal fragments (e.g. Sobotovich

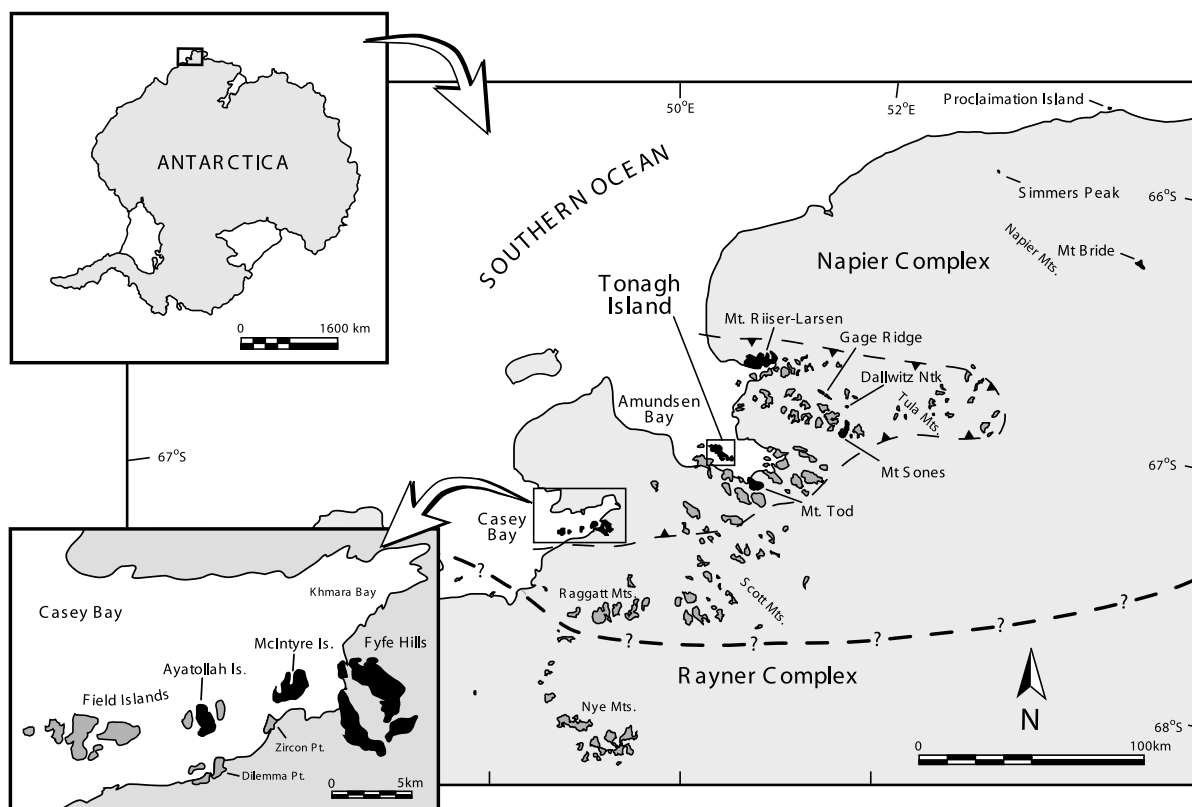


Fig. 1. Location of Tonagh Island (indicated in box) within Archaean Napier Complex. Various localities discussed in the text are highlighted and labelled. Boundary between Napier and Rayner Complexes (dashed with question marks) after Harley and Black (1987) and Harley and Hensen (1990). Regional extent of sapphirine + quartz assemblages delineated by dashed line with barbs (after Harley and Motoyoshi, 2000); the area enclosed within this line also approximately delineates the areal extent of UHT metamorphism. Upper inset: location of Napier Complex within Antarctic continent. Lower inset: enlargement of Casey Bay region, with localities discussed in text (from Black et al., 1983a).

et al., 1976; Lovering, 1979) and was refined and developed by subsequent work (e.g. DePaolo et al., 1982; Black et al., 1983a,b, 1986a,b; Harley and Black, 1997). Much of the research conducted since the early 1980's has focused on the construction of a structural-metamorphic timeframe for the evolution of the Napier Complex.

The generally adopted chronological scheme was largely developed by L.P. Black and coworkers during the early to mid 1980's, with subsequent refinement by Harley and Black (1997), the results of which are summarised here. Initial constraints on the timing of D_1 were based on a Rb–Sr whole-rock isochron age of 3072 ± 34 Ma (Sheraton and Black, 1983) from a syn- S_1 orthogneiss from Proclamation Island (Fig. 1), a location somewhat distal to the region of extreme metamorphism recorded in the Tula Mountains and Amundsen Bay regions to the SW. Based on these data, a number of workers maintained that UHT metamorphism occurred around this time (Black and James, 1983; Black et al., 1983a,b, 1986a,b). This estimate was later reassessed by the SHRIMP study of Harley and Black (1997) who concluded that UHT metamorphism and UHT-related D_1 could be no older than ~ 2840 Ma, based largely on the emplacement age of a syn- D_1 orthogneiss at Dallwitz nunatuk, located within the region of UHT metamorphism. They proposed a best estimate of 2837 ± 15 Ma for the timing of 'highest grade metamorphism', evaluated on zircon populations from three widely spaced samples.

The timing of D_2 has been subject to some uncertainty. Initially, the timing of D_2 was largely based on a Rb–Sr whole rock isochron age of $2840 + 220/-280$ Ma (Black et al., 1986a) from a granite body at Mt Bride (Fig. 1) for which a syn- D_2 emplacement age was inferred. An U–Pb zircon age of $2948 + 38/-17$ Ma from Mt Sones is also considered to represent an event at this time (Black et al., 1986b; Black, 1988). Other, less well-constrained, U–Pb ages have also been used as evidence to constrain the timing of D_2 . These include a concordant population of zircon ion probe U–Pb ages from a paragneiss from Mt Riiser-Larsen and a population of conventional U–Pb analyses from Mt Tod and Dallwitz Nuna-

tak (Black and James, 1983), all of which indicate evidence of an event at ~ 2900 Ma. Harley and Black (1997) revised these earlier estimates on the timing of D_2 based on their additional zircon data and stated that the entire D_1 – D_2 evolution may have been achieved during the time interval of 2850–2820 Ma, followed by an extended period of near-isobaric cooling.

Black et al. (1983a) presented conventional U–Pb analyses and centimetre-scale whole-rock Rb–Sr isochrons from felsic gneisses sampled from the Casey Bay region (Fig. 1) which record evidence for an event at ~ 2450 – 2480 Ma. Black et al. (1983a,b) concluded that these data indicate resetting of Rb–Sr systems, zircon growth and extensive resetting of the U–Pb system in pre-existing zircon during D_3 , the effects of which are pervasive in Casey Bay. A conventional zircon U–Pb age from a syn- D_3 pegmatite (Ayatollah Island; Fig. 1), yielded an upper intercept of $2456 + 8/-5$ Ma (Black et al., 1983a); a date that has become widely accepted as the best estimate for the timing of D_3 (Black and James, 1983; Black et al., 1983a,b, 1986a,b; Sheraton et al., 1987; Harley and Black, 1997). Numerous studies, using a variety of isotopic systems across the Napier Complex, report ages similar or identical to this value and these have been interpreted as representing isotopic disturbance during D_3 .

However, the above chronological scheme for the evolution of D_1 – D_3 has not been universally accepted. While there is little dispute concerning the antiquity of various protoliths across the Napier Complex, a number of authors have expressed an alternative view for the timing of the UHT metamorphism and structural evolution (Grew and Manton, 1979; Grew et al., 1982; Grew, 1998; DePaolo et al., 1982). These authors maintain that the timing of UHT metamorphism can be readily explained in terms of a short-lived metamorphic event at ~ 2450 – 2480 Ma (Grew, 1998), in contrast to the much earlier D_1 – D_2 tectonothermal evolution indicated above (Harley and Black, 1987, 1997). This alternative view evolved primarily over differing interpretations of syn-tectonic pegmatites in the Casey Bay region (Fig. 1). The syn- D_3 pegmatite dated by Black et al. (1983a); $2456 + 8/-5$ Ma) is instead inter-

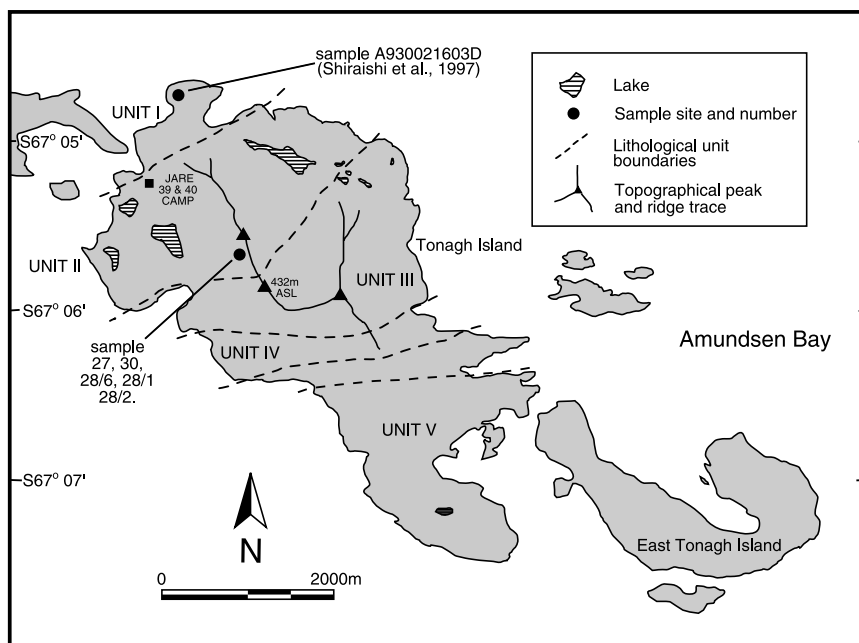


Fig. 2. Sample localities on Tonagh Island, including the sample site of Shirashi et al. (1997). Lithological subdivision boundaries (dashed and labelled) after Osanai et al. (1999).

puted to date UHT metamorphism based on the preservation of UHT mineral assemblages in structurally similar pegmatites (Grew, 1998). Sandiford and Wilson (1984) also suggest that such pegmatites were emplaced during D_2 boudinage, during UHT conditions. In this contribution, we document new zircon ion probe U–Pb data from a felsic orthogneiss exposed on central Tonagh Island and provide additional constraint on the timing of UHT metamorphism and of subsequent events that affected the Napier Complex.

3. Tonagh Island orthogneiss

Tonagh Island, the site of this study, is located in Amundsen Bay, south-western Napier Complex (Fig. 1). The geology of Tonagh Is. has been described in detail by Osanai et al. (1999) and, like the majority of the Napier Complex, comprises a variety of felsic to intermediate orthogneisses, minor mafic and ultramafic granulites and subordinate layered paragneiss sequences that include quartzites and ironstones. Osanai et al. (1999) also

subdivided the island into five lithological subdivisions (units I–V). These units represent coherent blocks of rock associations, the boundaries of which are marked by steeply dipping to vertical shear zones of unknown age.

One sample (sample 27) for U–Pb zircon analysis was taken from an orthopyroxene-bearing quartzo-feldspathic orthogneiss (after the map unit of Osanai et al., 1999; hereafter called the Tonagh Island orthogneiss in this contribution), the location of which is shown in Fig. 2. This unit is common on Tonagh Island and is light brown- to buff-coloured, homogeneous in appearance, containing an intense S_1 gneissosity defined by 1–10 mm scale subtle discontinuous, quartzo-feldspathic rich segregations. Typically the unit contains anhedral quartz ($\sim 35\%$ mode), K-feldspar ($\sim 14\%$) and plagioclase ($\sim 22\%$) and large (~ 2 – 3 mm diameter) subhedral mesoperthite (10–20%), orthopyroxene (3–5%) and minor clinopyroxene ($< 1\%$), with accessory ilmenite-magnetite, apatite, zircon and rare monazite (typically as mantles on apatite). A typical chemical analysis is listed in Table 1 (sample 27) and is further discussed below.

In addition to sample 27, multiple samples were collected from an alteration selvage or zone immediately adjacent to an Early Palaeozoic pegmatite. The location of samples collected from the alteration selvage (30, 28/6, 28/1 and 28/2) are illustrated in Fig. 3. Within the alteration selvage, the pyroxene-bearing orthogneiss had been extensively re-hydrated and recrystallised by aqueous fluids that accompanied pegmatite emplacement, resulting in replacement of pyroxene with biotite–hornblende–epidote assemblages at upper amphibolite facies

Table 1
Chemical composition of Tonagh Island orthogneiss

| Oxides | Sample 27 |
|---------------------------------|-----------|
| SiO ₂ | 71.08 |
| TiO ₂ | 0.44 |
| Al ₂ O ₃ | 14.05 |
| Fe ₂ O ₃ | 3.19 |
| MnO | 0.04 |
| MgO | 0.90 |
| CaO | 2.86 |
| Na ₂ O | 3.29 |
| K ₂ O | 3.67 |
| P ₂ O ₅ | 0.14 |
| LOI | 0.32 |
| Total | 99.98 |
| <i>Trace</i> | |
| Ba | 1355 |
| Nb | 6 |
| Rb | 69 |
| Sr | 257 |
| Y | 13 |
| Zr | 167 |
| Ce (0.1) | 90.0 |
| U (0.1) | 0.4 |
| Th (0.1) | 5.8 |
| Pb (2) | 14 |
| K/Rb | 220.7 |
| Ce _N /Y _N | 15.5 |
| Th/U | 14.5 |

Bulk rock geochemistry was conducted using XRF, conducted by X-ray assay laboratories (XRAL) in Don Mills, Ont., Canada. Major elements were determined on fused glass discs, trace elements (Ba, Nb, Rb, Sr, Y and Zr) on pressed powder pellets and Ce, U, Th and Pb determined by ICPMS techniques (detection limits shown). Results shown are average of two samples for major and trace elements, from one sample for ICPMS elements.

conditions (Carson et al., 2002). These samples were collected originally in order to assess the effect of Early Palaeozoic aqueous fluid influx on the host orthogneiss zircon population, the results of which have been presented in Carson et al. (2002). However, additional data and further assessment of the zircon U–Pb data of Carson et al. (2002) is presented here within the context of the regional chronological evolution of the Napier Complex.

4. Analytical procedures

Zircons were extracted from bulk hand samples (~5 kgs) and were separated using standard heavy liquid and magnetic techniques, mounted in epoxy, together with zircon standard AS3, (near concordant TIMS ²⁰⁶Pb/²³⁸U age of 1099.1 ± 0.5 Ma; Paces and Miller, 1993). The mounted grains were equatorially sectioned, polished and Au-coated. Backscattered electron (BSE) imaging was conducted to assess internal zircon structure and to facilitate selection of analysis sites (Fig. 4a–h) and were obtained using the JEOL JXA-8600 electron microprobe located at Yale University. Zircon U–Pb ion microprobe analyses were conducted on a CAMECA IMS 1270, located at the Department of Earth and Space Sciences, University of California, Los Angeles, USA. The analytical protocols for zircon analysis are summarized in Quidelleur et al. (1997). All isotopic ratios were corrected, where necessary, for common lead using measured ²⁰⁴Pb. Common Pb ratios used are ²⁰⁶Pb/²⁰⁴Pb = 16.2, ²⁰⁷Pb/²⁰⁴Pb = 15.35. Uranium and Th concentrations were estimated semi-quantitatively using U/⁹⁴Zr₂O and Th/⁹⁴Zr₂O in unknowns relative to that of the AS3 standard and normalised against published U and Th concentrations (Paces and Miller, 1993). Data reduction and processing were performed using ZIPS v2.4.1 (C.D. Coath 2000, unpublished software) and ISOPLOT v2.3 of Ludwig (1999).

Zircon U–Pb isotope results have been previously published in part (Carson et al., 2002; alteration zone samples 28/6, 28/1 and 28/2; unaltered protolith, sample 27; Fig. 3).

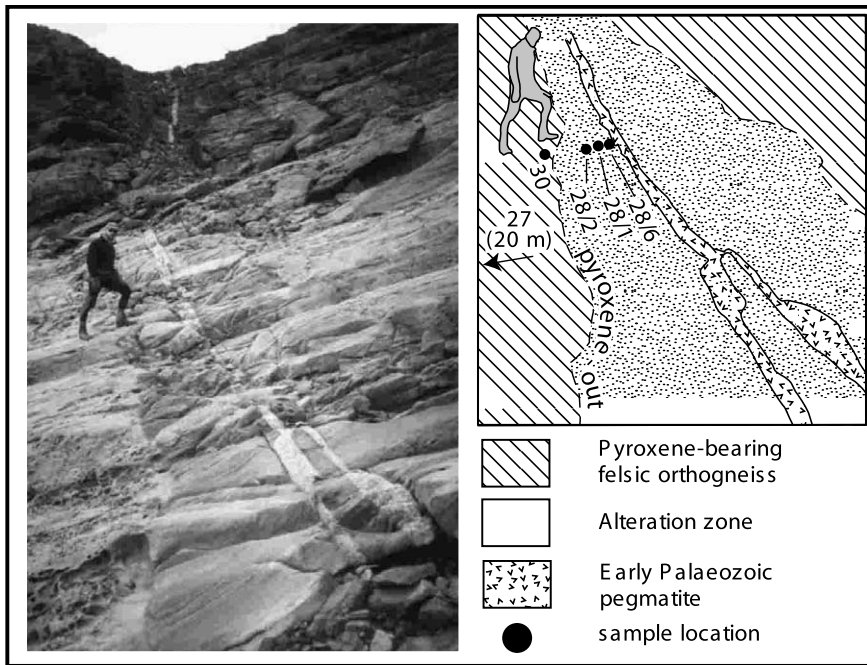


Fig. 3. Photograph and sketch map of sample site within the Tonagh Island orthogneiss adjacent to an Early Palaeozoic pegmatite. Note conspicuous 'bleach' zone adjacent to pegmatite (see also Carson et al., submitted for publication). The visible outer boundary of alteration zone indicates pyroxene-out isograd in the host orthogneiss. Samples 28/6, 28/1 and 28/2, 30 are 10, 160, 300 and 1100 mm respectively from left margin of the pegmatite; sample 27, 20 m to the left of pegmatite out of photograph. Photographer facing east, geologist for scale, sample location $67^{\circ}05'37.3''\text{S}$, $050^{\circ}17'09.8''\text{E}$.

We now evaluate these data presented by Carson et al. (2002) within the context of the regional geochronological evolution of the Napier Complex, and present additional isotopic data (Tables 2–4). Errors ellipses shown in Figs. 5–9 are at the one sigma level, weighted mean and intercept ages quoted are at the two sigma level and include U decay constant uncertainties.

5. Results

Zircons from the protolith and the alteration selvage have similar morphologies. Most common are euhedral to subhedral, clear to honey coloured grains, ~ 100 – $250\ \mu\text{m}$ in length, that have aspect ratios of ~ 2 – 3 . Under back scattered electron imaging, sectioned grains may exhibit fractured well defined cores which may show micron-scale oscillatory zoning (Fig. 4a

and b). Typically this core region is overgrown by a volumetrically dominant mantle, which although generally homogeneous (Fig. 4b and c), may exhibit oscillatory zoning at the micron scale (Fig. 4d). The mantle may crosscut the core regions (Fig. 4a) but more typically shows a conformable relationship with them. Another major population consists of anhedral spherical glassy 'gem-like' pinkish grains, up to 20 – $500\ \mu\text{m}$ in diameter (Fig. 4g and h), which display minimal structural development, and lack a clearly defined euhedral core or micron scale oscillatory zoning, although some coarse (10 – $20\ \mu\text{m}$) zoning may be present (Fig. 4g). A narrow ($< 20\ \mu\text{m}$), low U outer rim is typically present on most zircons (Fig. 4a–g) and may crosscut delicate oscillatory zoning present in the mantle (Fig. 4c and d). In total, 133 U–Pb analyses were conducted on 70 zircon grains; Tables 2–4 summarise the isotopic data.

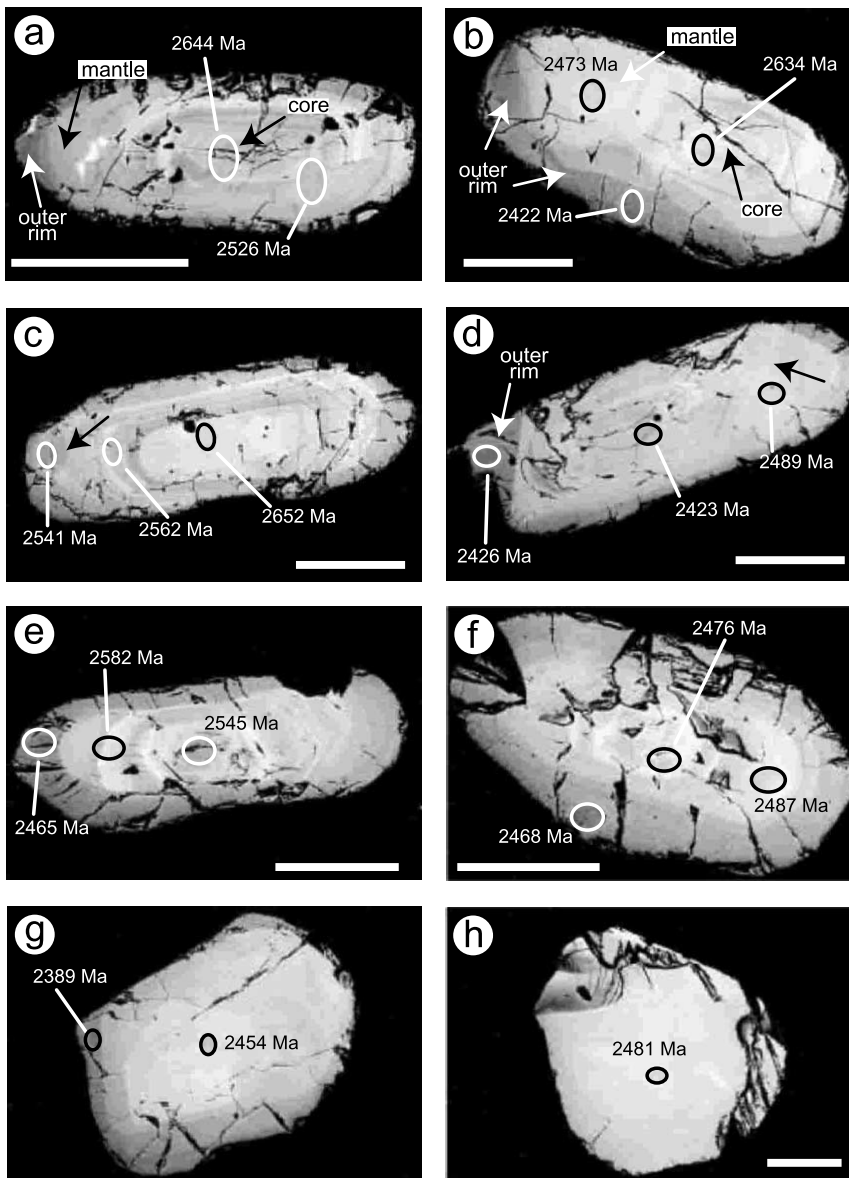


Fig. 4. BSE images of representative zircon morphologies. All annotated ages are $^{207}\text{Pb}/^{206}\text{Pb}$ ages, which may differ from upper intercept ages quoted in the text depending on degree of discordance, scale bar in all images = 100 μm : (a) sample number 28/2, grain 3, (disc 1), note zoned ~ 2600 Ma core, overgrown by faintly zoned mantle and outer rim. Analysis point with 2526 Ma age rejected due to overlap with significantly older core; (b) sample number 28/2, grain 6 (disc 1), finely zoned ~ 2600 Ma core, overgrown by wide homogeneous mantle which grades into dark outer rim; (c) sample number 28/3 grain 14 (disc 1), unzoned ~ 2600 Ma core, overgrown by zoned mantle and outer rim with ~ 2550 Ma ages. Note the transgressive nature of the outer rim at the arrowed location; (d) sample 28/1, grain 5 (disc 7). Finely zoned core (reset to ~ 2423 Ma?) overgrown by mantle and outer rim, outer rim appears to truncate mantle (e) sample 28/1, grain 7 (disc 7), coarsely zoned ~ 2550 Ma euhedral core over grown by outer rim; (f) sample number 28/2, grain 1 (disc 7) (g) sample number 27, grain 14 (disc 1), anhedral grain with coarse concentric zoning. (h) sample 28/6, grain 15 (disc 7). Homogeneous anhedral grain with negligible zoning.

Table 2
U–Pb ages and isotopic compositions of selected zircon cores from Tonagh Island, Amundsen Bay

| Age (Ma) $^{206}\text{Pb}/^{238}\text{U}$ | ± | Age (Ma) $^{207}\text{Pb}/^{235}\text{U}$ | ± | Age (Ma) $^{207}\text{Pb}/^{206}\text{Pb}$ | ± | % $^{206}\text{Pb}^*$ | $^{207}\text{Pb}^*/^{235}\text{U}$ | ± | $^{206}\text{Pb}^*/^{238}\text{U}$ | ± | $^{207}\text{Pb}^*/^{206}\text{Pb}^*$ | ± | Th/U | Disc. % | U (ppm) | Th (ppm) | Date\ sample # disc # grain # .spot # | Spot location |
|--|------|--|------|---|------|-----------------------|------------------------------------|-------|------------------------------------|---------|---------------------------------------|----------|------|---------|---------|----------|--|-----------------|
| 2607 | 25.5 | 2594 | 11.6 | 2585 | 10.5 | 99.7 | 11.870 | 0.146 | 0.4983 | 0.00593 | 0.1728 | 0.001080 | 0.4 | 100.9 | 748 | 332 | 2000-2Dec\ 281.dl.gr12.sp1 | Defined core |
| 2558 | 33.9 | 2589 | 17.8 | 2614 | 14.7 | 99.4 | 11.800 | 0.224 | 0.4870 | 0.00783 | 0.1758 | 0.001560 | 0.3 | 97.9 | 765 | 221 | 2000-2Dec\ 281.dl.gr15.sp1 | Defined core |
| 2553 | 25.5 | 2601 | 15.5 | 2639 | 14.6 | 99.3 | 11.960 | 0.198 | 0.4859 | 0.00588 | 0.1785 | 0.001570 | 0.1 | 96.7 | 523 | 68 | 2000-2Dec\ 281.dl.gr16.sp1 | Defined core |
| 2584 | 30.2 | 2598 | 16.9 | 2609 | 15.9 | 99.5 | 11.920 | 0.216 | 0.4931 | 0.00700 | 0.1753 | 0.001670 | 0.9 | 99.0 | 384 | 360 | 2000-2Dec\ 281.dl.gr8.sp1 | Defined core |
| 2371 | 37.2 | 2521 | 19.4 | 2644 | 11.8 | 99.4 | 10.970 | 0.229 | 0.4445 | 0.00833 | 0.1790 | 0.001270 | 0.5 | 89.7 | 410 | 237 | 2000-2Dec\ 282.dl.gr3.sp1 | Defined core |
| 2583 | 59.1 | 2612 | 26.4 | 2634 | 12.6 | 99.6 | 12.100 | 0.340 | 0.4929 | 0.01370 | 0.1780 | 0.001350 | 0.8 | 98.1 | 568 | 479 | 2000-2Dec\ 282.dl.gr6.sp1 | Defined core |
| 2478 | 46.5 | 2554 | 25.4 | 2614 | 24.2 | 99.0 | 11.370 | 0.309 | 0.4688 | 0.01060 | 0.1759 | 0.002550 | 0.6 | 94.8 | 249 | 151 | 2000-2Dec\ 282.dl.gr8.sp1 | Defined core |
| 2698 | 20.7 | 2672 | 10.2 | 2652 | 10.2 | 99.6 | 12.900 | 0.139 | 0.5198 | 0.00487 | 0.1799 | 0.001100 | 0.4 | 101.7 | 838 | 399 | 2000-2Dec\ 283.dl.gr14.sp1 | Defined core |

% $^{206}\text{Pb}^*$ denotes percentage of radiogenic ^{206}Pb ; uncertainties are given at the 1σ level. U and Th contents are semiquantitative estimates based on $\text{U}/^{206}\text{Pb}$ and $\text{Th}/^{206}\text{Pb}$ relative to that of measured values of AS3 standard and published U and Th concentrations. Disc. % is the individual discordance = $(^{206}\text{Pb}/^{238}\text{U} \text{ age} - ^{207}\text{Pb}/^{206}\text{Pb} \text{ age}) / ^{207}\text{Pb}/^{206}\text{Pb} \text{ age} \times 100$, 100% = concordant analysis.

Table 3
U–Pb ages and isotopic compositions of selected zircons from Tonagh Island, Amundsen Bay

| Age (Ma) $^{206}\text{Pb}/^{238}\text{U}$ | ± | Age (Ma) $^{207}\text{Pb}/^{235}\text{Ua}$ | ± | Age (Ma) $^{206}\text{Pb}/^{238}\text{Pb}$ | ± | % $^{206}\text{Pb}^*$ | $^{207}\text{Pb}^*/^{235}\text{U}$ | ± | $^{206}\text{Pb}^*/^{238}\text{U}$ | ± | $^{207}\text{Pb}^*/^{206}\text{Pb}^*$ | ± | Th/U | Disc.% | U (ppm) | Th (ppm) | Date\ sample # disc # grain # spot # | Spot location |
|--|------|---|------|---|------|-----------------------|------------------------------------|-------|------------------------------------|---------|---------------------------------------|----------|------|--------|------------|-------------|---|------------------|
| 2667 | 23.1 | 2600 | 9.72 | 2548 | 6.35 | 99.9 | 11.940 | 0.124 | 0.5125 | 0.00542 | 0.1690 | 0.000640 | 0.5 | 104.7 | 1121 | 617 | 2000-30Nov\ 282.d7.gr11.sp3 | Defined core |
| 2593 | 20.7 | 2558 | 9.34 | 2529 | 9.51 | 99.7 | 11.410 | 0.114 | 0.4953 | 0.00480 | 0.1671 | 0.000947 | 1.1 | 102.5 | 685 | 813 | 2000-30Nov\ 282.d7.gr12.sp2 | Defined core |
| 2643 | 20.3 | 2590 | 10.1 | 2548 | 6.54 | 99.5 | 11.810 | 0.128 | 0.5067 | 0.00475 | 0.1690 | 0.000660 | 1.0 | 103.7 | 654 | 700 | 2000-30Nov\ 282.d7.gr16.sp2 | Defined core |
| 2626 | 22.3 | 2578 | 9.05 | 2540 | 7.91 | 99.8 | 11.660 | 0.113 | 0.5029 | 0.00520 | 0.1682 | 0.000794 | 0.5 | 103.4 | 655 | 331 | 2000-30Nov\ 282.d7.gr6.sp2 | Defined core |
| 2481 | 19.4 | 2519 | 12.4 | 2550 | 10.7 | 99.5 | 10.950 | 0.146 | 0.4695 | 0.00443 | 0.1692 | 0.001080 | 0.1 | 97.3 | 562 | 72 | 2000-30Nov\ 283.d7.gr1.sp1 | Mantle |
| 2542 | 25.9 | 2543 | 14.1 | 2545 | 13.7 | 98.3 | 11.240 | 0.170 | 0.4833 | 0.00595 | 0.1687 | 0.001380 | 0.3 | 99.9 | 327 | 97 | 2000-1Dec\ 281.d7.gr7.sp1 | Defined core |
| 2485 | 33.4 | 2515 | 17.7 | 2539 | 15.8 | 99.4 | 10.900 | 0.207 | 0.4703 | 0.00763 | 0.1681 | 0.001580 | 0.1 | 97.9 | 682 | 58 | 2000-2Dec\ 281.d1.gr3.sp3 | Mantle |
| 2549 | 24.0 | 2563 | 12.9 | 2574 | 8.72 | 99.5 | 11.480 | 0.158 | 0.4850 | 0.00552 | 0.1717 | 0.000896 | 0.4 | 99.0 | 897 | 439 | 2000-2Dec\ 283.d1.gr14.sp2 | Mantle |
| 2598 | 32.9 | 2566 | 17.2 | 2542 | 11.2 | 99.4 | 11.520 | 0.212 | 0.4963 | 0.00764 | 0.1684 | 0.001130 | 0.1 | 102.2 | 500 | 57 | 2000-2Dec\ 286.d1.gr10.sp1 | Defined core |
| 2360 | 36.1 | 2450 | 17.3 | 2526 | 14.2 | 99.5 | 10.170 | 0.190 | 0.4420 | 0.00808 | 0.1668 | 0.001410 | 0.3 | 93.4 | 575 | 213 | 2000-2Dec\ 282.d1.gr3.sp2 | Mantle |

% $^{206}\text{Pb}^*$ denotes percentage of radiogenic ^{206}Pb , uncertainties are given at the 1σ level. U and Th contents are semi-quantitative estimates based on $\text{U}/^{207}\text{Pb}$ and $\text{Th}/^{207}\text{Pb}$ relative to that of measured values of AS3 standard and published U and Th concentrations. Disc.% is the individual discordance = $(^{206}\text{Pb}/^{238}\text{U} \text{ age} - 1 \times 100) + 100$, 100% = concordant analysis.

Table 4
U-Pb ages and isotopic compositions of selected zircons from Tonagh Island, Amundsen Bay

| Age (Ma) $^{238}\text{Pb}/^{235}\text{U}$ | \pm | Age (Ma) $^{238}\text{Pb}/^{235}\text{U}$ | \pm | Age (Ma) $^{207}\text{Pb}/^{206}\text{Pb}$ | \pm | % $^{206}\text{Pb}^*$ | $^{207}\text{Pb}^*/^{235}\text{U}$ | \pm | $^{206}\text{Pb}^*/^{238}\text{U}$ | \pm | $^{207}\text{Pb}^*/^{206}\text{Pb}^*$ | \pm | Th/U | Disc.% | U (ppm) | Th (ppm) | Date\ sample # disc # grain # spot # | Spot location |
|--|-------|--|-------|---|-------|-----------------------|------------------------------------|-------|------------------------------------|---------|---------------------------------------|---------|------|--------|------------|-------------|---|------------------|
| 2462 | 81.7 | 2465 | 39.6 | 2468 | 24.4 | 99.0 | 10.340 | 0.442 | 0.4650 | 0.01860 | 0.1612 | 0.00233 | 3.2 | 99.8 | 78 | 277 | 2000-30Nov\ 282.d7.gr1.sp3 | Outer rim |
| 2324 | 57.7 | 2364 | 50.5 | 2398 | 69.3 | 97.5 | 9.256 | 0.510 | 0.4340 | 0.01280 | 0.1547 | 0.00630 | 3.2 | 96.9 | 76 | 267 | 2000-30Nov\ 282.d7.gr11.sp1 | Outer rim |
| 2400 | 48.5 | 2416 | 34.8 | 2430 | 57.1 | 97.9 | 9.798 | 0.370 | 0.4510 | 0.01090 | 0.1576 | 0.00531 | 1.0 | 98.8 | 111 | 114 | 2000-30Nov\ 282.d7.gr11.sp2 | Outer rim |
| 2476 | 77.2 | 2461 | 43.3 | 2449 | 41.0 | 97.7 | 10.290 | 0.481 | 0.4683 | 0.01760 | 0.1594 | 0.00386 | 2.8 | 101.1 | 65 | 196 | 2000-30Nov\ 282.d7.gr16.sp1 | Outer rim |
| 2570 | 75.2 | 2518 | 44.0 | 2476 | 46.9 | 97.8 | 10.940 | 0.518 | 0.4899 | 0.01740 | 0.1620 | 0.00450 | 2.1 | 103.8 | 60 | 136 | 2000-30Nov\ 282.d7.gr8.sp1 | Outer rim |
| 2666 | 62.1 | 2549 | 27.1 | 2457 | 25.3 | 98.4 | 11.310 | 0.328 | 0.5122 | 0.01460 | 0.1601 | 0.00240 | 1.2 | 108.5 | 154 | 209 | 2000-30Nov\ 282.d7.gr9.sp2 | Outer rim |
| 2590 | 91.6 | 2489 | 55.3 | 2408 | 67.0 | 97.5 | 10.610 | 0.632 | 0.4946 | 0.02120 | 0.1555 | 0.00613 | 4.0 | 107.6 | 47 | 206 | 2000-30Nov\ 283.d7.gr1.sp2 | Outer rim |
| 2692 | 29.2 | 2586 | 20.9 | 2504 | 25.9 | 98.4 | 11.760 | 0.262 | 0.5182 | 0.00689 | 0.1646 | 0.00253 | 1.5 | 107.5 | 163 | 271 | 2000-30Nov\ 283.d7.gr10.sp3 | Outer rim |
| 2514 | 62.6 | 2497 | 31.8 | 2484 | 23.8 | 98.8 | 10.700 | 0.366 | 0.4769 | 0.01430 | 0.1627 | 0.00229 | 1.0 | 101.2 | 167 | 179 | 2000-30Nov\ 283.d7.gr16.sp1 | UG |
| 2258 | 43.5 | 2363 | 44.3 | 2455 | 60.8 | 97.6 | 9.254 | 0.447 | 0.4195 | 0.00957 | 0.1600 | 0.00576 | 3.3 | 92.0 | 94 | 338 | 2000-30Nov\ 283.d7.gr18.sp2 | Outer rim |
| 2380 | 41.8 | 2399 | 24.5 | 2416 | 29.4 | 98.7 | 9.622 | 0.256 | 0.4465 | 0.00939 | 0.1563 | 0.00270 | 3.4 | 98.5 | 94 | 347 | 2000-30Nov\ 283.d7.gr19.sp1 | UG |
| 2350 | 70.2 | 2417 | 49.9 | 2474 | 55.1 | 97.7 | 9.807 | 0.531 | 0.4398 | 0.01570 | 0.1617 | 0.00528 | 2.6 | 95.0 | 94 | 267 | 2000-30Nov\ 283.d7.gr3.sp2 | Outer rim |
| 2449 | 68.2 | 2471 | 47.3 | 2488 | 55.2 | 97.7 | 10.390 | 0.531 | 0.4622 | 0.01550 | 0.1631 | 0.00534 | 3.6 | 98.4 | 76 | 303 | 2000-30Nov\ 283.d7.gr4.sp2 | Outer rim |
| 2523 | 56.8 | 2473 | 39.3 | 2433 | 37.6 | 98.2 | 10.420 | 0.442 | 0.4790 | 0.01300 | 0.1578 | 0.00350 | 2.9 | 103.7 | 100 | 314 | 2000-30Nov\ 283.d7.gr5.sp2 | Mantle |
| 2526 | 61.9 | 2499 | 35.5 | 2477 | 36.7 | 98.1 | 10.720 | 0.409 | 0.4798 | 0.01420 | 0.1620 | 0.00353 | 2.3 | 102.0 | 78 | 193 | 2000-30Nov\ 283.d7.gr7.sp2 | Mantle |
| 2542 | 69.5 | 2506 | 59.0 | 2477 | 72.8 | 97.0 | 10.800 | 0.686 | 0.4834 | 0.01600 | 0.1621 | 0.00700 | 6.5 | 102.6 | 49 | 352 | 2000-30Nov\ 286.d7.gr10.sp1 | Core of UG |

Table 4 (continued)

| Age (Ma) $^{206}\text{Pb}/^{238}\text{U}$ | Age (Ma) $^{207}\text{Pb}/^{235}\text{U}$ | Age (Ma) $^{207}\text{Pb}/^{235}\text{U}$ | \pm | Age (Ma) $^{207}\text{Pb}/^{235}\text{U}$ | \pm | % $^{206}\text{Pb}^*$ | $^{207}\text{Pb}^*/^{235}\text{U}$ | \pm | $^{206}\text{Pb}^*/^{238}\text{U}$ | \pm | $^{207}\text{Pb}^*/^{235}\text{U}$ | \pm | Th/U | Disc.% | U (ppm) | Th (ppm) | Date\ sample # disc # grain # spot # | Spot location |
|--|--|--|-------|--|-------|-----------------------|------------------------------------|-------|------------------------------------|---------|------------------------------------|---------|------|--------|------------|-------------|---|--------------------|
| 2421 | 75.1 | 2412 | 57.9 | 2404 | 81.4 | 96.1 | 9.752 | 0.613 | 0.4557 | 0.01700 | 0.1552 | 0.00744 | 5.8 | 100.7 | 36 | 228 | 2000-30Nov\ 286.d7.gr10.sp2 | Outer rim of UG |
| 2555 | 18.2 | 2493 | 8.2 | 2442 | 4.6 | 99.9 | 10.650 | 0.094 | 0.4865 | 0.00420 | 0.1587 | 0.00043 | 0.1 | 104.6 | 1617 | 135 | 2000-30Nov\ 286.d7.gr5.sp1 | Outer rim |
| 2488 | 44.1 | 2455 | 23.0 | 2427 | 19.8 | 99.3 | 10.220 | 0.254 | 0.4710 | 0.01010 | 0.1573 | 0.00184 | 0.8 | 102.5 | 214 | 178 | 2000-30Nov\ 282.d7.gr12.sp1 | Outer rim |
| 2535 | 13.6 | 2478 | 7.1 | 2432 | 6.0 | 100.0 | 10.480 | 0.080 | 0.4818 | 0.00312 | 0.1577 | 0.00056 | 0.1 | 104.2 | 2367 | 328 | 2000-30Nov\ 283.d7.gr10.sp1 | Reset core |
| 2499 | 56.7 | 2457 | 24.8 | 2424 | 22.4 | 99.3 | 10.250 | 0.275 | 0.4734 | 0.01300 | 0.1570 | 0.00208 | 1.1 | 103.1 | 205 | 251 | 2000-30Nov\ 283.d7.gr10.sp4 | Outer rim |
| 2485 | 33.3 | 2466 | 19.3 | 2450 | 19.5 | 99.0 | 10.340 | 0.215 | 0.4703 | 0.00759 | 0.1594 | 0.00184 | 1.4 | 101.4 | 168 | 254 | 2000-30Nov\ 283.d7.gr5.sp3 | Outer rim |
| 2440 | 16.8 | 2436 | 8.3 | 2433 | 5.0 | 99.9 | 10.010 | 0.090 | 0.4600 | 0.00381 | 0.1579 | 0.00047 | 0.1 | 100.3 | 1611 | 242 | 2000-30Nov\ 283.d7.gr7.sp1 | Reset core |
| 2607 | 39.0 | 2536 | 28.1 | 2479 | 33.9 | 98.5 | 11.150 | 0.336 | 0.4984 | 0.00906 | 0.1623 | 0.00326 | 2.2 | 105.2 | 175 | 415 | 2000-1Dec\ 281.d7.gr20.sp2 | Outer rim |
| 2592 | 98.9 | 2497 | 63.8 | 2421 | 78.2 | 96.3 | 10.700 | 0.735 | 0.4949 | 0.02290 | 0.1568 | 0.00722 | 2.5 | 107.1 | 58 | 155 | 2000-1Dec\ 281.d7.gr5.sp3 | Outer rim |
| 2484 | 42.0 | 2474 | 25.3 | 2465 | 31.4 | 98.2 | 10.430 | 0.285 | 0.4701 | 0.00958 | 0.1609 | 0.00299 | 2.0 | 100.8 | 115 | 246 | 2000-1Dec\ 281.d7.gr7.sp3 | Outer rim |
| 2385 | 70.2 | 2440 | 36.2 | 2485 | 21.6 | 98.8 | 10.050 | 0.394 | 0.4478 | 0.01580 | 0.1628 | 0.00208 | 1.3 | 96.0 | 170 | 246 | 2000-1Dec\ 282.d7.gr8.sp2 | UG |
| 2529 | 93.9 | 2502 | 68.9 | 2481 | 81.3 | 96.7 | 10.760 | 0.797 | 0.4804 | 0.02160 | 0.1624 | 0.00783 | 5.9 | 101.9 | 57 | 365 | 2000-1Dec\ 286.d7.gr15.sp1 | UG |
| 2448 | 52.7 | 2459 | 39.4 | 2468 | 44.1 | 98.1 | 10.270 | 0.437 | 0.4620 | 0.01200 | 0.1612 | 0.00421 | 1.0 | 99.2 | 188 | 202 | 2000-2Dec\ 281.d1.gr15.sp2 | Outer rim |
| 2547 | 56.6 | 2516 | 45.5 | 2490 | 50.4 | 98.0 | 10.910 | 0.533 | 0.4846 | 0.01300 | 0.1633 | 0.00489 | 2.2 | 102.3 | 137 | 325 | 2000-2Dec\ 281.d1.gr16.sp3 | Outer rim |
| 2393 | 48.3 | 2432 | 24.7 | 2465 | 22.8 | 99.0 | 9.973 | 0.267 | 0.4495 | 0.01090 | 0.1609 | 0.00217 | 0.7 | 97.1 | 255 | 185 | 2000-2Dec\ 281.d1.gr8.sp3 | Outer rim |
| 2523 | 102.0 | 2468 | 63.6 | 2423 | 65.9 | 96.2 | 10.370 | 0.712 | 0.4789 | 0.02350 | 0.1570 | 0.00610 | 4.7 | 104.1 | 56 | 294 | 2000-2Dec\ 286.d1.gr10.sp2 | Mantle |

Table 4 (continued)

| Age (Ma) ^{238}U | \pm | Age (Ma) ^{235}U | \pm | Age (Ma) ^{206}Pb | \pm | $\%^{206}\text{Pb}^*$ | $^{207}\text{Pb}^*/^{235}\text{U}$ | \pm | $^{206}\text{Pb}^*/^{238}\text{U}$ | \pm | $^{207}\text{Pb}^*/^{206}\text{Pb}^*$ | \pm | Th/U | Disc.% | U (ppm) | Th (ppm) | Date/ sample # disc # grain # spot # | Spot location |
|------------------------------|-------|------------------------------|-------|-------------------------------|-------|-----------------------|------------------------------------|-------|------------------------------------|---------|---------------------------------------|---------|------|--------|------------|-------------|---|------------------|
| 2363 | 29.8 | 2419 | 18.2 | 2466 | 20.5 | 99.3 | 9.829 | 0.194 | 0.4428 | 0.00667 | 0.1610 | 0.00196 | 0.7 | 95.8 | 459 | 350 | 2000-2Dec\ 286.dl.gr4.sp3 | Outer rim |
| 2365 | 23.4 | 2407 | 15.8 | 2442 | 19.2 | 99.3 | 9.701 | 0.167 | 0.4432 | 0.00523 | 0.1587 | 0.00180 | 0.9 | 96.8 | 378 | 370 | 2000-2Dec\ 281.dl.gr3.sp2 | Outer rim |
| 2404 | 73.8 | 2465 | 39.5 | 2517 | 45.1 | 98.2 | 10.340 | 0.441 | 0.4519 | 0.0166 | 0.1659 | 0.00445 | 6.0 | 95.5 | 64 | 420 | 2000-2Dec\ 27.dl.gr1.sp1 | Mantle |
| 2357 | 42.1 | 2432 | 21.3 | 2496 | 16.0 | 99.3 | 9.970 | 0.231 | 0.4413 | 0.00941 | 0.1638 | 0.00156 | 1.5 | 94.4 | 270 | 438 | 2000-2Dec\ 27.dl.gr1.sp2 | UG |
| 2438 | 71.9 | 2412 | 47.2 | 2389 | 60.0 | 97.0 | 9.752 | 0.499 | 0.4597 | 0.0163 | 0.1539 | 0.00542 | 5.7 | 102.1 | 60 | 374 | 2000-2Dec\ 27.dl.gr14.sp2 | Outer rim |
| 2433 | 32.8 | 2479 | 17.3 | 2516 | 13.4 | 99.3 | 10.490 | 0.196 | 0.4586 | 0.00743 | 0.1658 | 0.00132 | 1.4 | 96.7 | 361 | 554 | 2000-2Dec\ 27.dl.gr3.sp1 | UG |
| 2406 | 58.6 | 2428 | 35.9 | 2447 | 43.0 | 98.4 | 9.927 | 0.386 | 0.4524 | 0.0132 | 0.1591 | 0.00404 | 1.5 | 98.3 | 116 | 186 | 2000-2Dec\ 27.dl.gr3.sp2 | Mantle |
| 2436 | 50.7 | 2464 | 25.1 | 2488 | 20.3 | 99.2 | 10.330 | 0.280 | 0.4593 | 0.0115 | 0.1631 | 0.00197 | 1.2 | 97.9 | 273 | 359 | 2000-2Dec\ 27.dl.gr9.sp1 | UG |
| 2505 | 44.0 | 2477 | 19.6 | 2454 | 11.5 | 99.7 | 10.470 | 0.221 | 0.4748 | 0.0101 | 0.1599 | 0.00109 | 0.9 | 102.1 | 384 | 394 | 2000-2Dec\ 27.dl.gr14.sp1 | UG |
| 2399 | 31.9 | 2422 | 16.9 | 2442 | 14.3 | 99.4 | 9.866 | 0.180 | 0.4509 | 0.00718 | 0.1587 | 0.00134 | 0.8 | 98.2 | 349 | 310 | 2000-2Dec\ 27.dl.gr2.sp1 | UG |

$^{206}\text{Pb}^*$ denotes percentage of radiogenic ^{206}Pb ; uncertainties are given at the 1σ level; UG, anhedral unstructured grain. U and Th contents are semi-quantitative estimates based on $\text{U}/^{92}\text{Zr}_2\text{O}$ and $\text{Th}/^{92}\text{Zr}_2\text{O}$ relative to that of measured values of AS3 standard and published U and Th concentrations. Disc.% is the individual discordance = $(^{206}\text{Pb}/^{238}\text{U} \text{ age} - ^{207}\text{Pb}/^{235}\text{U} \text{ age}) / ^{206}\text{Pb} \text{ age} - 1 \times 100 + 100$, 100% = concordant analysis.

A subgroup of analyses (eight analyses from eight grains) have $^{207}\text{Pb}/^{206}\text{Pb}$ ages between ~ 2600 – 2650 Ma (Fig. 5; Table 3). These analyses are all from texturally well-defined zircon cores (e.g. Fig. 4a–c), and have U and Th contents between ~ 250 – 840 ppm and ~ 70 – 480 ppm respectively, with Th/U of between 0.1–0.9. Analyses from this population range from slightly reversely discordant (102%, one analysis), to normally discordant (90%). The data approximates a linear trend (MSWD = 4.7) with an upper concordia intercept of 2626 ± 28 Ma and a very imprecise lower intercept of 164 ± 1200 Ma.

Another small subgroup of analyses (10 analyses from 10 grains) has $^{207}\text{Pb}/^{206}\text{Pb}$ ages between ~ 2529 – 2575 Ma (Fig. 6; Table 3). Analysis sites of this population are well defined variably-zoned cores (Fig. 4e) or mantles that overgrow cores of ~ 2600 Ma age (Fig. 4c). Uranium and Th contents are variable, ~ 320 – 1100 ppm and ~ 60 – 810 ppm respectively, with Th/U ranging

from 0.1–1.1. This population displays a range from reversely to normally discordant with a maximum of 104–93%, respectively. An error weighted regression (MSWD = 2.1) gives an upper concordia intercept of 2546 ± 13 Ma, with an imprecise lower intercept of 45 ± 640 Ma.

Most analyses form a population with $^{207}\text{Pb}/^{206}\text{Pb}$ ages around ~ 2450 – 2470 Ma (Fig. 7; Table 4 and including previously published data from Carson et al., 2002). Many of these analyses are from mantles and low-U outer rim sites, although several are from defined cores and may represent isotopically reset magmatic cores (Fig. 4d). No concordant age could be calculated for these data (Ludwig, 1998), but they form a near linear trend, with some excess scatter, for which an error weighted regression ($n = 115$, MSWD = 4.0) gives an upper concordia intercept of 2476.9 ± 9 Ma with a lower intercept of 531 ± 200 Ma. In further considering these data, we subdivided these analyses into ei-

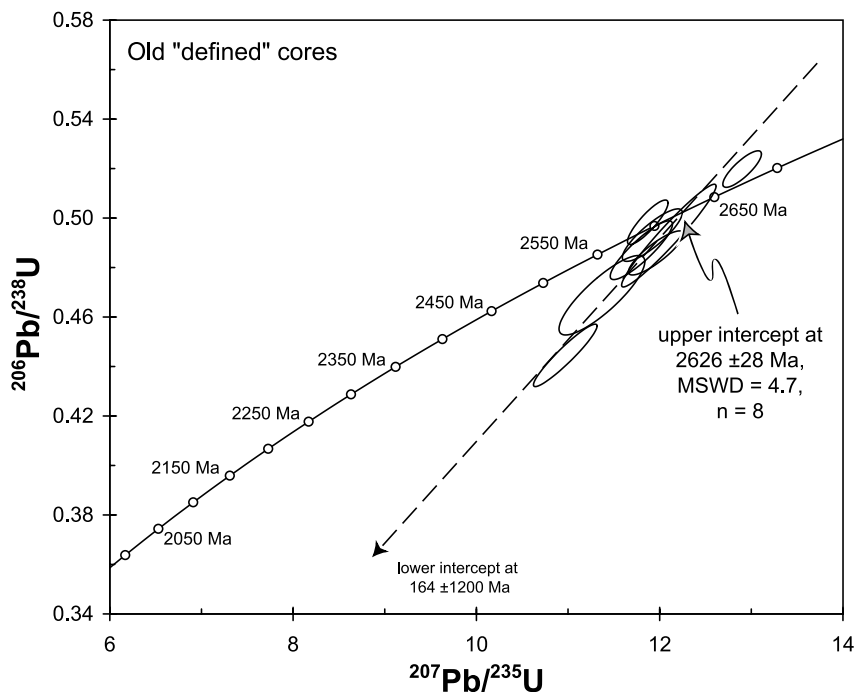


Fig. 5. Conventional concordia diagram showing zircon U–Pb isotope data from a population of old well-defined cores (Fig. 4a–c). Line is an error-weighted regression with an upper intercept of 2626 ± 28 Ma and a poorly defined lower intercept of 164 ± 1200 Ma.

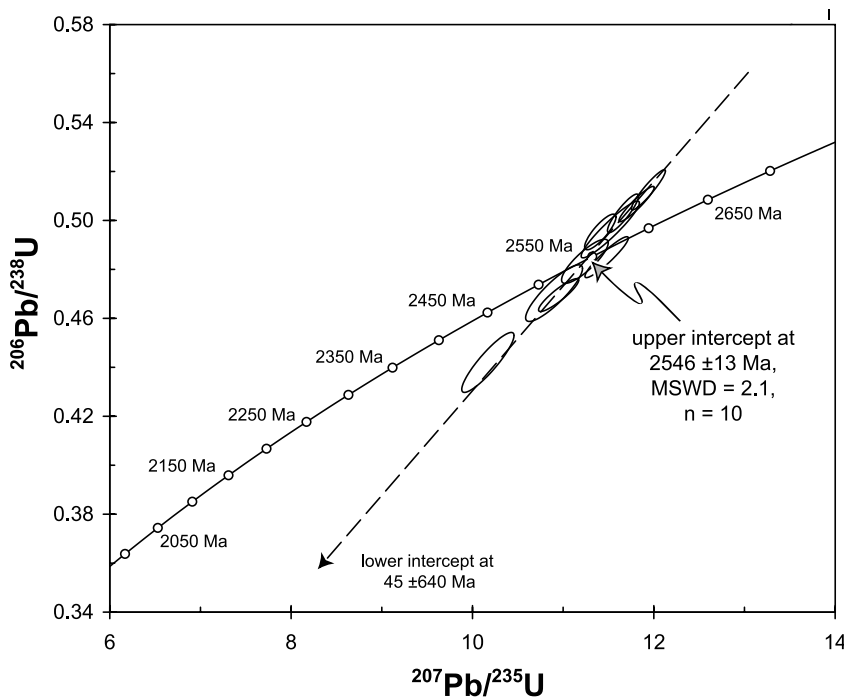


Fig. 6. Conventional concordia diagram showing zircon U–Pb isotope data from a selected population of analyses that form an error-weighted regression with an upper intercept of 2546 ± 13 Ma and a poorly defined lower intercept of 45 ± 640 Ma.

ther high Th/U types or outer rims (which may include analyses with high Th/U). Analyses with high Th/U (> 1.2) define a linear trend with an error weighted regression with no excess scatter ($n = 52$, $\text{MSWD} = 1.03$) and an upper concordia intercept of 2483.0 ± 9 Ma (Fig. 8). Common Pb is typically higher in analyses with elevated Th/U, and with lower U contents (Table 2). High Th/U analysis sites are commonly broad mantles, but may also include occasional narrow outer rims and, less commonly, indistinct unzoned cores. All low U outer rims (with ‘dark’ BSE response; Fig. 4b–g), regardless of Th/U, were regressed together and show a linear trend with no excess scatter ($n = 24$, $\text{MSWD} = 0.67$) and an upper intercept of 2455 ± 16 Ma (Fig. 9). It is tempting to suggest that the narrow outer rims may represent the later stage of a progression of zircon growth (~ 2455 Ma) which commenced with the growth of the high Th/U group at ~ 2483 Ma. Treatment as separate populations is supported by a MSWD of < 1 for each group (high Th/U and the outer rim groups) when regressed separately.

6. Discussion

Prior to discussing the zircon isotopic data below, it is appropriate to deliberate on the chemical characteristics of the Tonagh Island orthogneiss (Table 1). Sheraton and Black (1983) made two broad distinctions of felsic to intermediate orthogneiss units within the Napier Complex, ‘undepleted’ and ‘depleted’ varieties, the latter defined by strong depletion of a variety of elements and also on the basis of various elemental ratios, including Th/U and chondrite normalised Ce_N/Y_N . Sheraton and Black (1983) concluded that depleted varieties acquired their particular geochemical signature primarily as a result of partial melting of a garnet-bearing mafic source, rather than resulting from UHT metamorphism, though this effect was also considered. This geochemical discrimination was used by Sheraton and Black (1983) to characterise intrusive suites that pre-dated UHT metamorphism. However, it should be stressed that chemical sig-

natures alone cannot provide a robust criteria for assessing orthogneiss emplacement relative to UHT metamorphism. The purpose of the following geochemical information is to further describe the nature of the orthogneiss under investigation. In presenting this data, we do not imply any timing relationships of orthogneiss emplacement relative to UHT conditions.

The Tonagh Island orthogneiss illustrates many of the defining characteristics of ‘depleted’ orthogneisses. This unit has low values of Y relative to TiO_2 (cf. Fig. 10 of Sheraton and Black (1983)), low Th (5.8 ppm) and U (0.4 ppm) and very high Th/U (14.5; Fig. 13 of Sheraton and Black (1983)). Relative to SiO_2 , Ce, Nb, Ti, Zr, Rb and Y all are comparable with the depleted orthogneiss fields shown in Fig. 5 of Sheraton and Black (1983). Based on these geochemical characteristics, we

conclude that the Tonagh Island orthogneiss belongs to the ‘depleted’ class of felsic orthogneisses defined by Sheraton and Black (1983).

The small population of clearly defined zircon cores ($n=8$) with an upper intercept age of 2626 ± 28 Ma (Fig. 5) has Th/U values typically around 0.3–0.5 (with three analyses at 0.1, 0.8 and 0.9), values typical of magmatic zircon (Maas et al., 1992). It is also significant to note that there are no ages older than ~ 2650 Ma in 133 analyses of 70 zircon grains from this orthogneiss, precluding any significant prior geological history. The magmatic values of Th/U, together with the well-defined, micron-scale oscillatory zoned nature of the cores suggests an igneous origin. We conclude that the emplacement of this voluminous ‘depleted’ felsic intrusive on Tonagh Island occurred at 2626 ± 28 Ma.

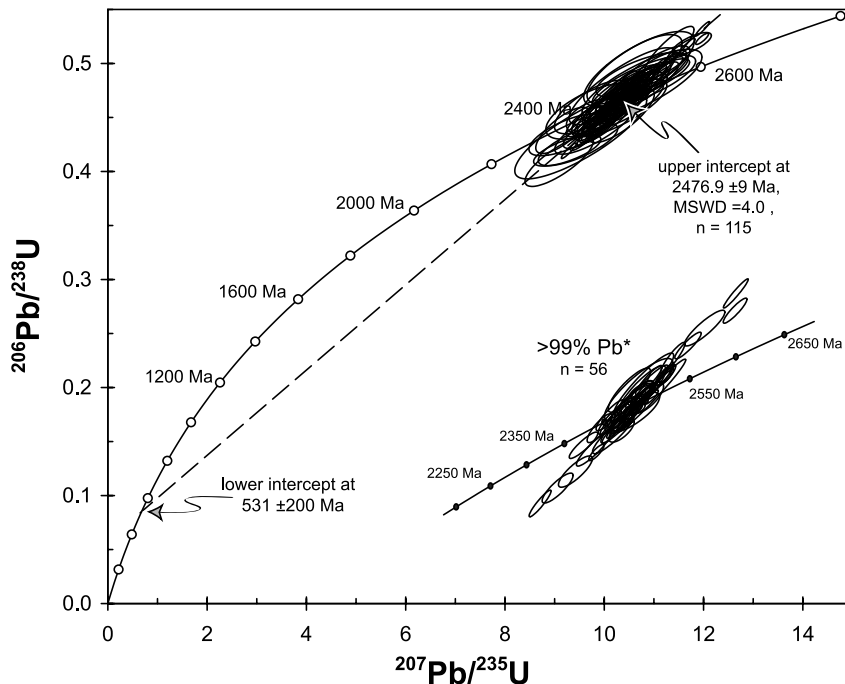


Fig. 7. Conventional concordia diagram showing all remaining zircon U–Pb isotope data. These data approximate a linear trend ($n=115$; $\text{MSWD}=4.0$) and an error-weighted regression yield an upper intercept of 2476.9 ± 9 Ma and a lower intercept of 531 ± 200 Ma. The diagram is visually dominated by 59 analyses with large error ellipses; such analyses typically include high Th/U and low U outer rims, that have elevated common Pb levels and have correspondingly large Pb/U errors. The high Th/U and low U outer rim analyses are separately treated in Figs. 8 and 9 respectively. The inset at lower right shows a selected subset ($n=56$) of U–Pb analyses with Pb^* contents $> 99\%$ and correspondingly smaller errors.

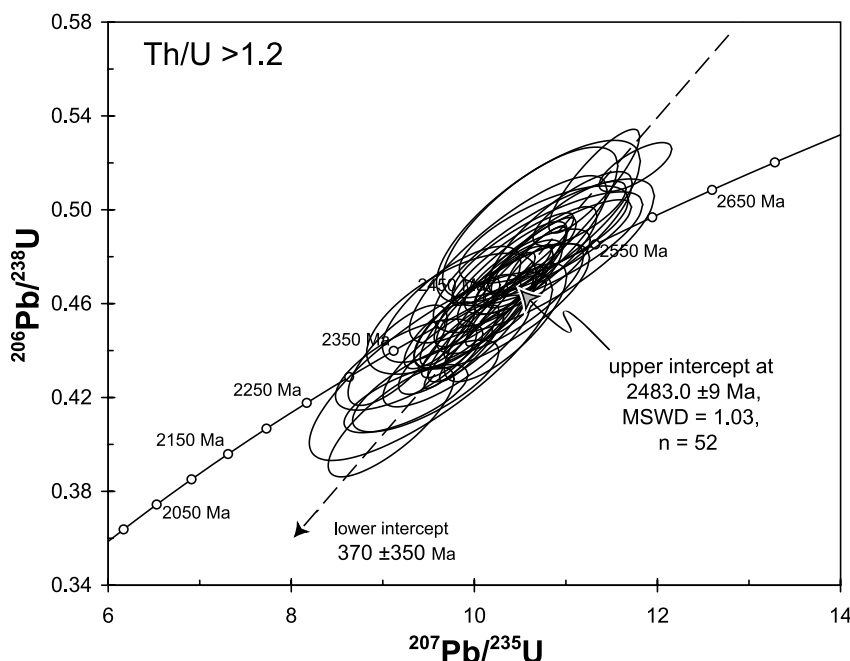


Fig. 8. Conventional concordia diagram showing zircon U–Pb isotope data from high Th/U (>1.2) analyses, a subdivision of the data presented in Fig. 7. These analyses form an error-weighted regression, with no excess scatter ($n = 52$; $\text{MSWD} = 1.03$) with an upper intercept of 2483.0 ± 9 Ma and a poorly defined lower intercept of 370 ± 350 Ma.

The population of ages with an upper concordia intercept of 2546 ± 13 Ma (Fig. 6) is somewhat problematic. Shirashi et al. (1997) also noted a small population of zircons with $^{207}\text{Pb}/^{206}\text{Pb}$ ages ~ 2550 Ma in their analysis of a quartz-feldspar gneiss from layered paragneiss sequence on northern Tonagh Island (Fig. 2), but were unclear on the significance of these. They speculated that the population may represent an episode of new zircon growth. Recent SHRIMP analysis on zircons extracted from a leucosome from McIntyre Is (Fig. 1) also yield U–Pb ages of 2560–2590 Ma (S.L. Harley; unpublished data). The growth of new zircon is also suggested at this time (S.L. Harley personal communication). These interpretations are consistent with our observations in that analysis sites that yield ~ 2550 Ma represent either cores (Fig. 4e) or overgrowths (Fig. 4c) on older ~ 2600 Ma cores. We acknowledge that there was a period of new zircon growth at 2546 ± 13 Ma, with formation of new grains and overgrowths on ~ 2600 Ma cores, but main-

tain that the geological significance of this period of zircon growth is currently unclear given the limited geological and isotopic information on this event.

6.1. Significance of the 2450–2470 Ma ages and the timing of UHT metamorphism

The majority of zircon U–Pb analyses from this study form a population that have an upper concordia intercept ~ 2450 – 2470 Ma, statistically identical with many isotopic ages from across the Napier Complex. Partial resetting of old zircon U–Pb systems from orthogneiss protoliths results in (generally imprecise) lower intercepts at ~ 2400 – 2500 Ma (Black and James, 1983; Williams et al., 1984; Black et al., 1986a,b; Harley and Black, 1997), interpreted to indicate a period of major isotopic disruption. Upper intercepts of other zircon populations also commonly indicate ages of ~ 2450 – 2470 Ma, which has been interpreted as a period of zircon growth or of the

complete resetting of pre-existing zircon (e.g. Black et al., 1983a, 1986a,b). Rb–Sr and Sm–Nd whole-rock isochrons ages also indicate a period of extensive isotopic re-equilibration at this time (e.g. Black and James, 1983; Black et al., 1983a; Black and McCulloch, 1987; Owada et al., 1994; Tainosho et al., 1994, 1997). The interpretation of this strong isotopic signature at ~ 2450 – 2480 Ma, recorded from a wide variety of rock types and isotopic systems is critical to models of the geochronological-metamorphic framework of the Napier Complex.

Black et al. (1983a), for example, maintained that the widespread and strong isotopic signature at ~ 2460 Ma is due to the pervasive effects of D_3 and recrystallisation associated with the development of S_3 , and that the D_1 – D_2 and UHT evolution occurred ~ 400 Ma earlier, during the mid to late Archaean. In contrast, Grew (1998) acknowledges that while all studies seem to agree that isotopic systems were highly disturbed and reset at ~ 2450 – 2480 Ma, he questions the assertion

that UHT metamorphism occurred ~ 400 Ma earlier. Grew (1998) maintains that the timing of UHT metamorphism can be readily explained in terms of a short-lived metamorphic event at ~ 2450 – 2480 Ma in contrast to the much earlier D_1 – D_2 tectonothermal evolution preferred by Harley and Black (1987, 1997). This alternative interpretation is largely based on the preservation of UHT assemblages within ‘syn- D_3 ’ pegmatites (Grew, 1998) and syn- D_2 UHT pegmatites (Grew et al., 1982; Sandiford and Wilson, 1984; Sandiford and Powell, 1986b) both of which yield upper intercept ages of ~ 2500 Ma (Grew et al., 1982). These contrasting interpretations must be addressed within the context of the presently available data and take into account the following facts.

(1) In the Field Islands (Fig. 1) the effects of D_3 are reported to be locally intense (Black et al., 1983a) and proceeded at upper-amphibolite facies conditions (650 – 720 °C and 5 – 8 kbar; Harley and Black, 1987). This D_3 event is thought to

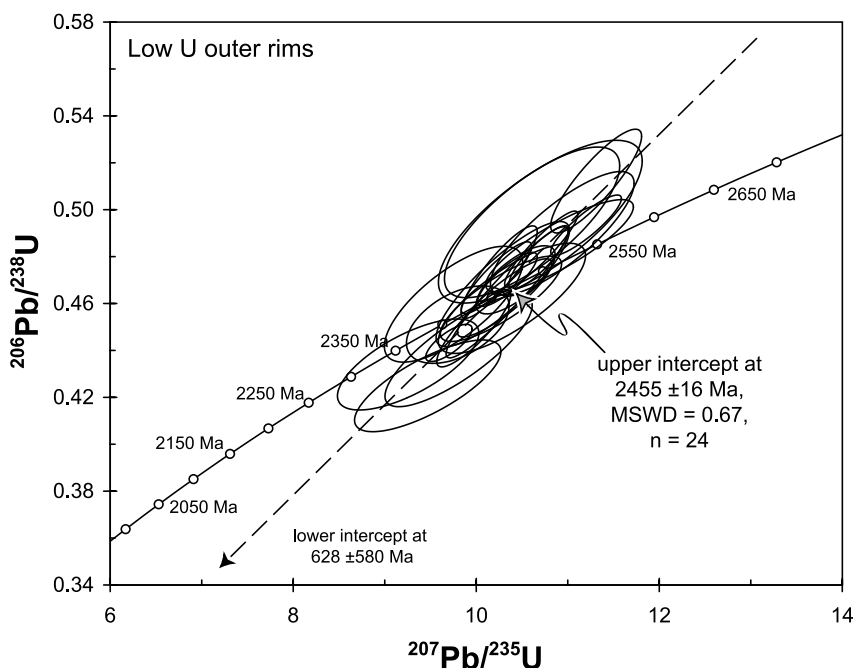


Fig. 9. Conventional concordia diagram showing zircon U–Pb isotope data from low U outer rim analyses only, a subdivision of the data presented in Fig. 7. These analyses form an error-weighted regression, with no excess scatter ($n = 24$; $MSWD = 0.67$) with an upper intercept of 2455 ± 16 Ma and a poorly defined lower intercept of 628 ± 580 Ma.

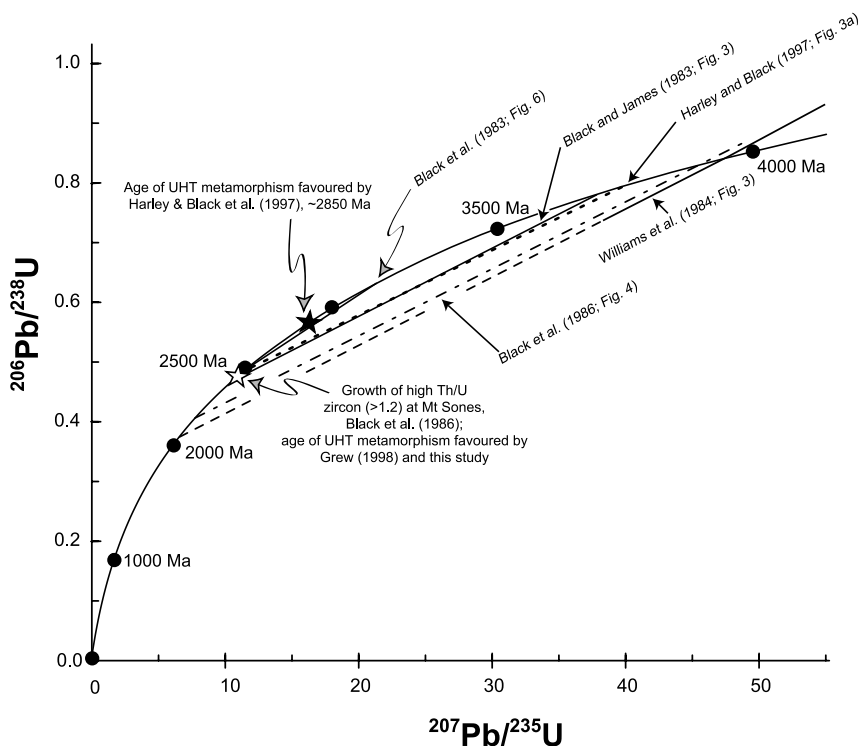


Fig. 10. Summary concordia diagram of the U–Pb isotopic results from two pre-UHT orthogneiss units (Tonalitic Gneiss, Mt Sones, Black and James, 1983; Williams et al., 1984; Harley and Black, 1997; and a charnockitic leucogneiss from Fyfe Hills, Black and James, 1983). Of importance here is the lack of disturbance at the timing of UHT metamorphism (~ 2820 – 2850 Ma) favoured by Harley and Black (1997); indicated by the solid star). Although the lower intercept indicated by the study of Williams et al. (1984) is somewhat younger than ~ 2500 Ma (2030 ± 170 Ma), that study concluded the lower intercept was the likely result of disturbance during an event at ~ 2400 Ma, but did not elaborate on the nature of that event.

have been responsible for extensive resetting of Rb–Sr whole-rock and U–Pb zircon systematics at ~ 2450 – 2480 Ma. However, intensity of D_3 across the Napier Complex is quite varied, yet this strong isotopic imprint at ~ 2450 – 2480 Ma is almost always present. At the sample location for this study (Fig. 3), for example, there is no local penetrative fabric development or any deformation that can be attributed to D_3 , yet the upper intercept age for the majority of analyses presented here ranges between 2455–2483 Ma.

(2) The sampled orthogneiss on Tonagh Island contains a pervasive, generally flat-lying gneissosity, S_1 , that parallels a S_1 gneissosity that is defined by UHT assemblages in adjacent paragneiss sequences. The orthogneiss also contains abundant (10–20% modal) mesoperthite. These

observations suggest that the orthogneiss was emplaced into the crust prior to UHT conditions, and subsequently endured the entire D_1 – D_2 structural evolution, including UHT metamorphism. Since orthogneiss emplacement, based on the data presented here, occurred at 2626 ± 28 Ma, UHT metamorphism and D_1 cannot be older than this.

(3) A more general observation from the numerous isotopic studies is that a number of zircon U–Pb systems, which date the emplacement of pre- D_1 /UHT orthogneiss units, show little or no isotopic disturbance at the timing of UHT conditions favoured by either Black et al. (1983a) or Harley and Black (1997) (Black and James, 1983, Fig. 3; Black et al., 1983b, 1986b, Fig. 6; Williams et al., 1984, Fig. 3; Fig. 4; Harley and Black, 1997, Fig. 3a and b). These units

instead show discordia with (albeit imprecise) lower intercepts consistent with disturbance at ~ 2400 – 2500 Ma (Fig. 10).

Based on our data and observations, UHT metamorphism must have post-dated emplacement of the Tonagh Island orthogneiss at 2626 ± 28 Ma. There are two periods of zircon growth subsequent to 2626 ± 28 Ma identified in this study, one at 2546 ± 13 Ma and again at 2476.9 ± 9 Ma (taking the weighted mean of all analyses of ~ 2450 – 2480 Ma as shown in Fig. 7); UHT metamorphism must have occurred during one of these episodes. Given the intense isotopic disturbance in a number of isotopic systems across the entire Napier Complex at ~ 2450 – 2480 Ma and the absence of any significant D_3 effects at the sample locality (point 1), we propose that UHT metamorphism and D_1 – D_2 , at least in the Tonagh Island region, occurred at ~ 2450 – 2480 Ma, supporting the assertion of Grew (1998). We acknowledge that the growth of zircon at 2546 ± 13 Ma may indicate a metamorphic episode at this time. However, we discount the possibility that UHT metamorphism occurred at this time, given the paucity of data of ~ 2550 Ma from presently available chronological studies of the Napier Complex.

Our conclusion contrasts with the structurally-constrained chronological framework presented by, for example, Harley and Black (1997) which argues for UHT metamorphism at 2850 – 2820 Ma. The timing of syn- D_1 felsic intrusives, in particular the Dallwitz Nunatak orthogneiss (~ 2850 Ma), is central to the calibration of the revised chronological framework of Harley and Black (1997). In order to reconcile these differences, one might argue for multiple episodes of UHT metamorphism across the Napier Complex. An episode of UHT metamorphism that peaked in the eastern periphery of the Tula Mountains at 2850 Ma (Harley and Black, 1997) may have been post-dated by a younger episode of UHT metamorphism at ~ 2470 Ma in the Amundsen Bay region, and which also exerted a strong isotopic overprint across the terrane and cumulated in the regional development of upright D_3 fold structures at upper amphibolite grade. This suggestion would imply that the D_1 – D_2 structural features between the eastern Tula Mountains and Amund-

sen Bay are not time equivalents, although this presents no particular geological difficulty.

Indeed, the possibility of high-grade polymetamorphism in the Napier Complex has been previously explored by Hensen and Motoyoshi (1992) and Harley and Black (1997). In one proposal, Hensen and Motoyoshi (1992) suggested that separate overprinting high temperature events may offer a better explanation for petrological features associated with D_1 and D_2 at Mt Riiser-Larsen (Fig. 1), considering that the time span originally proposed for the D_1 – D_2 evolution (~ 3072 – 2850 Ma) is considered too long to sustain temperatures in excess of 900 °C (Harley and Hensen, 1990). Harley and Black (1997) also address the possibility of multiple tectonothermal events. Those authors propose that a high-grade fabric forming event at $\sim 2980 \pm 9$ Ma, synchronous with their revised timing of emplacement of the Proclamation Island orthogneiss, occurred in northern regions of the terrane. This fabric forming event was superseded by D_1 – D_2 and UHT metamorphism in the Tula-Scott mountains region, at 2850 – 2820 Ma, the time of UHT favoured by Harley and Black (1997). While these discussions do not directly relate to the suggestion offered here, in that UHT metamorphism in the Amundsen Bay region at ~ 2470 Ma post-dated an earlier episode UHT metamorphism in the Tula-Scott mountains region at 2850 – 2820 Ma, they do indicate willingness of researchers to address the possibility of polymetamorphic events in order to account for inconsistencies in the petrographic, chronological and structural framework for the Napier Complex.

In spite of the abundance of isotopic data collected in the Napier Complex, there remains insufficient data to fully test and assess the possibility of two UHT events, one at 2850 – 2820 Ma and another at ~ 2450 – 2480 Ma in the Amundsen Bay area. We believe that another difficulty with this suggestion is that it fails to explain point 3 above, in that some lithologies located in the eastern Tula Mountains, such as the Tonalitic Gneiss at Mt Sones and the Gage Ridge orthogneiss, show no clear evidence of isotopic disturbance at the timing of UHT metamorphism favoured by Harley and Black (1997). It would

seem unusual that UHT metamorphism at ~ 2850 Ma (Harley and Black, 1997), an event of extreme metamorphic conditions (>1100 °C) and intense pervasive deformation, across a considerable region, left an comparatively minor isotopic imprint and only in some rock types. In addition, one might argue that it seems equally unusual that D_3 , a relatively lower grade event (≤ 700 °C), with marked heterogeneous structural distribution, resulted in a widespread, remarkably consistent, strong isotopic imprint at ~ 2450 – 2480 Ma in virtually all rock types and isotopic systems (e.g. Sandiford and Wilson, 1984; Sheraton et al., 1987).

6.2. High Th/U zircons

An intriguing feature of the zircon data of Black et al. (1986b), and of this study, is the presence of a near concordant zircon population with an unusually high Th/U (>1.2). Many zircon analyses of the volumetrically dominant mantle and outer rims in this study have high Th/U (Table 4; Carson et al., 2002) which, if regressed as a separate population, yield an upper intercept age of 2483.0 ± 9 Ma ($n = 52$, Fig. 8). This age is identical to that reported by Black et al. (1986b) for a near concordant population of high Th/U (>1.2) ‘structureless crystals’ which yielded a ‘preferred’ $^{207}\text{Pb}/^{206}\text{Pb}$ mean age of 2479 ± 23 Ma. Although exhaustive studies of the processes and conditions controlling zircon Th/U remain to be conducted, in general, zircons grown under metamorphic conditions frequently have low Th/U, typically < 0.05 – 0.1 (Williams and Claesson, 1987; Maas et al., 1992). Indeed, reported Th/U values greater than unity are quite uncommon, and the high Th/U zircon population presented here, and in Black et al. (1986b), clearly indicates the formation of zircon in an unusual chemical environment. Black et al. (1986b) argued that the growth of zircon with such unusual chemistry is due to crystallisation in an environment depleted in U relative to Th. Those authors also argue that depletion must have occurred prior to crystallisation of this distinctive zircon population, during UHT metamorphism at 3070 Ma.

However, in a zircon U–Pb ion probe study of the Scandinavian Caledonides, Williams and Claesson (1987) concluded that the growth of zircon, with characteristically low Th/U, occurred during the transitional amphibolite–granulite Caledonian orogeny, at which time Th and U were mobilised. They discounted the alternative possibility that loss of Th and U from the host rock occurred prior to the growth of the low Th/U zircon. They based this on the observation that a spectrum of pre-existing Precambrian zircon grains, with ‘normal’ Th/U (typically 0.1 – 0.5), have Caledonian age lower intercepts, a period of metamorphism during which new zircon growth occurred, characterised by low Th/U (< 0.1).

Similarly, following Williams and Claesson (1987), we propose that the zircon population with high Th/U described here characterises zircon growth during UHT metamorphism. Although the example of Williams and Claesson (1987) specifically addresses the growth of low Th/U zircon during Palaeozoic metamorphism in the Scandinavian Caledonides, the logic of their conclusion is relevant here. We suggest that the actinides were mobilised during UHT metamorphism, with preferential extraction of U over Th from the terrane, providing a chemical environment during peak conditions that facilitated the growth of high Th/U zircon. Discordance trends in much older, >2470 Ma, pre-existing zircon populations reported in other U–Pb studies from the Napier Complex frequently have (albeit imprecise) lower intercepts that coincide with the growth of the high Th/U zircon population at ~ 2470 Ma (see point 3 above). We reaffirm, therefore, that the upper intercept age of 2483.0 ± 9 Ma for the high Th/U analyses (Fig. 8) may indicate the best estimate for the timing of UHT metamorphism.

The low U outer rims (Fig. 9) yield an upper intercept of 2455 ± 16 Ma, which is significantly distinct from the high Th/U zircon population (2483.0 ± 9 Ma). Zircon from the low U population are restricted to the outer margins of zircon grains (e.g. Fig. 4b–g) and are generally charac-

terised by low U (and relatively low Th) contents. The low U outer rims may result from zircon growth during continued U depletion of the terrane resulting from UHT metamorphism. Based on the textural context of the low U zircon (as rim material), we suggest that the low U outer rim zircon represents the final period of zircon growth that occurred during waning UHT metamorphism.

6.3. Reverse discordance

It should be noted that a number of the U–Pb analyses shown in Fig. 7 are reversely discordant. Although discussion of the significance of the observed reverse discordance for this dataset is presented elsewhere (Carson et al., 2002), a brief summary is offered here. Reverse discordance is considered to be either genuine, resulting from intragrain net excess of Pb* due to redistribution during a geological disturbance (e.g. Williams et al., 1984; Harley and Black, 1997) or an analytical artefact due to differential ionisation efficiencies between standard and unknown resulting in enhanced Pb ion yields (e.g. McLaren et al., 1994; Wiedenbeck, 1995). Carson et al. (submitted for publication) concluded that reverse discordance exhibited by a subset of the zircon population illustrated in Fig. 7 is genuine, based on a non-zero lower intercept, as defined by the spread of both normal and reversely discordant data, that coincides with a known episode of geological disturbance (Section 6.4), and evidence of sub-micron scale Pb and U heterogeneities. An analytical artefact rationale for the observed reverse discordance was discounted, primarily on the absence of a zero lower intercept; as a zero intercept is a characteristic feature of differing ionisation efficiencies between the standard and a set of unknowns (e.g. McLaren et al., 1995; Wiedenbeck, 1995). It should be noted, however, that regardless of the nature of reverse discordance, real or analytical artefact, the upper intercept age is still considered robust (Wiedenbeck, 1995), and the geochronological information derived from upper intercepts in this study remain valid.

6.4. Significance of post-2460 Ma lower intercept ages

The present study also permits some discussion of the significance of post-2460 Ma lower intercepts reported in many U–Pb studies of the Napier Complex. A number of imprecise U–Pb lower intercepts at ~1000 Ma have been documented from the Field Islands, near the boundary with the NeoProterozoic Rayner Complex (Fig. 1). These lower intercepts have been attributed to isotopic disturbance in response to ~1000 Ma granulite-facies tectonothermal activity in the adjacent Rayner Complex (Grew et al., 1982; Black et al., 1983a, 1986b; Sandiford and Wilson, 1984). However, Shirashi et al. (1997) re-examined the chronological evolution of the western-most regions of the Rayner Complex and showed that, immediately adjacent to the Napier Complex, the Rayner Complex experienced high-grade metamorphism during the Early Palaeozoic (~500–550 Ma). Shirashi et al. (1997) proposed that the western extremities of the Rayner Complex instead represent the eastward extension of the Early Palaeozoic Lützow–Holm Complex and that the western Rayner Complex may in fact represent a collage of NeoProterozoic and Early Palaeozoic terranes, including ~770 Ma felsic intrusive bodies. This scenario clearly introduces some complexity in the interpretation and significance of the ~1000 Ma lower intercept ages reported from within the Napier Complex.

Although, imprecise due to extended extrapolations to concordia, the U–Pb zircon analyses presented here (Fig. 7) indicate an Early Palaeozoic lower intercept (see also Grew and Manton, 1979). Carson et al. (2002) concluded that, for the orthogneiss studied here, zircon discordance was directly related to disturbance due to aqueous fluid infiltration, at upper-amphibolite grade (~8 kb and ~670 °C; Carson et al., submitted for publication), accompanying emplacement of an Early Palaeozoic pegmatite. This raises the possibility that post-2450 Ma concordia lower intercepts may result, at least in part, from isotopic disturbance due to aqueous fluid infiltration into the Napier Complex during the Early Palaeozoic, particularly for lithologies

where there is demonstrable hydration due to proximity to Early Palaeozoic pegmatites. For example, based on the description of the biotite-bearing 'grey gneiss' by Black et al. (1983a) from Ayatollah Island, Casey Bay, that unit is clearly related to the proximity of a large pegmatite body of Early Palaeozoic age (Rb–Sr whole-rock age of 522 ± 10 Ma; Black et al., 1983a). Almost certainly, the formation of this 'grey gneiss' resulted from hydration and recrystallisation of the anhydrous 'pink gneiss' by influx of aqueous fluids accompanying pegmatite emplacement (Grew and Manton, 1979; Carson et al., 2002). This conclusion is supported by a Rb–Sr whole-rock isochron from this 'grey gneiss' which yields a somewhat imprecise age of 650 ± 145 Ma (Black et al., 1983a). Although the lower intercept based on conventional U–Pb zircon analyses from this unit is $1183 + 433 / - 446$ Ma (Black et al., 1983a), a likely cause of zircon discordance is the influx of magmatic fluids due to the emplacement of the nearby Early Palaeozoic pegmatite. Although, some well-defined lower intercepts are clearly related to the effects of tectonothermal activity of Rayner age (Black et al., 1984), the interpretation of other less precise lower intercepts and 'geologically meaningless' lower intercepts (Black et al., 1986a, Fig. 7b and c) across the Napier Complex are problematic in this light, and should address the possibility of superimposed effects of fluid influx into the Napier Complex, during the Early Palaeozoic.

7. Conclusions

The zircon U–Pb data presented from Tonagh Island provide additional constraints on the timing of UHT metamorphism within the Napier Complex, East Antarctica, which has been a topic of debate for two decades. We conclude that:

- (a) the emplacement of a major felsic orthogneiss body on Tonagh Island, occurred at 2626 ± 28 Ma, prior to the onset of UHT metamorphism and intense D_1 – D_2 deformation.
- (b) Two episodes of zircon growth occurred subsequent to orthogneiss emplacement. A minor episode of growth occurred at 2546 ± 13 Ma,

followed by a major episode of growth commencing with the high Th/U mantles at 2483.0 ± 9 Ma and terminating with outer rim development at 2455 ± 16 Ma.

- (c) UHT metamorphism occurred, at least in the Tonagh Island region, synchronous with the growth of high Th/U zircon at 2483.0 ± 9 Ma, with zircon growth continuing at least until 2455 ± 16 Ma as represented by the growth of low-U outer rims. We find no compelling evidence that supports UHT metamorphism at either ~ 2840 or ~ 3070 Ma.
- (d) Post ~ 2460 Ma zircon lower intercepts reported from the Napier Complex are commonly considered to result from isotopic disturbance during adjacent Rayner Complex tectonothermal activity (~ 1000 Ma). We stress that such lower intercepts may also be complicated by isotopic disturbance due to aqueous fluid influx, at elevated conditions, into the Napier Complex which accompanied Early Palaeozoic pegmatite emplacement at ~ 500 Ma.

Acknowledgements

CJC acknowledges participation in the 40th Japanese Antarctic Research Expeditions and the SEAL (Structure and Evolution of East Antarctic Lithosphere) program, at the kind invitation of K. Shiraishi and Y. Motoyoshi of the National Institute of Polar Research, Tokyo. CJC also wishes to thank the expeditioners of JARE-39 and -40, particularly the Tonagh Island field party, and the officers and crew of the icebreaker Shirase, for the hospitality extended to him during JARE-40. Assistance by, and discussion with, T.M. Harrison, M. Grove, K. McKeegan and C.M. Breeding during ion probe sessions at the Department of Earth and Space Sciences, UCLA, and with J. Eckert during electron microprobe sessions at Yale University is appreciated. E.S. Grew provided the photograph in Fig. 3 and comments on early version of the manuscript. The manuscript benefited from valuable and constructive reviews from Simon Harley and an anonymous reviewer.

CJC acknowledges receipt of the Damon Wells fellowship at Yale University; analytical costs were supported by National Science Foundation grant EAR-0001084 and -9810089.

References

- Black, L.P., James, P.R., 1983. Geological history of the Archaean Napier Complex in Enderby Land. In: Oliver, R.L., James, P.R., Jago, J.B. (Eds.), *Antarctic Earth Science*. Cambridge University Press, Cambridge, pp. 11–15.
- Black, L.P., James, P.R., Harley, S.L., 1983a. Geochronology and geological evolution of metamorphic rocks in the Field Islands area, East Antarctica. *J. Metamorphic Geol.* 1, 277–303.
- Black, L.P., James, P.R., Harley, S.L., 1983b. The geochronology, structure and metamorphism of early Archaean rocks at Fyfe Hills, Enderby Lands, Antarctica. *Precambrian Res.* 21, 197–222.
- Black, L.P., Fitzgerald, J.D., Harley, S.L., 1984. Pb isotopic composition, colour, and microstructure of monazites from a polymetamorphic rock in Antarctica. *Contrib. Mineral Petrol.* 85, 141–148.
- Black, L.P., Sheraton, J.W., James, P.R., 1986a. Late Archaean granites of the Napier Complex, Enderby Land, Antarctica: a comparison of Rb–Sr, Sm–Nd and U–Pb isotopic systematics in a complex terrain. *Precambrian Res.* 32, 343–368.
- Black, L.P., Williams, I.S., Compston, W., 1986b. Four zircon ages from one rock: the history of a 3930 Ma old granulite from Mt Sones, Enderby Land, Antarctica. *Contrib. Mineral Petrol.* 94, 427–437.
- Black, L.P., McCulloch, M.T., 1987. Evidence for isotopic re-equilibration of Sm–Nd whole-rock systems in Early Archaean crust of Enderby Land, Antarctica. *Earth Planet Sci. Lett.* 82, 15–24.
- Black, L.P., Harley, S.L., Sun, S.S., McCulloch, M.T., 1987. The Rayner Complex of east Antarctica, Complex isotopic systematics within a Proterozoic mobile belt. *J. Metamorphic Geol.* 5, 1–26.
- Black, L.P., 1988. Isotopic resetting of U–Pb zircon and Rb–Sr and Sm–Nd whole-rock systems in Enderby Land, Antarctica: implications for the interpretation of isotopic data from polymetamorphic and multiply deformed terrains. *Precambrian Res.* 38, 355–365.
- Carson, C.J., Ague, J.J., Grove, M., Coath, C.D., Harrison, T.M., 2002. U–Pb isotopic behaviour of zircon during upper-amphibolite facies fluid infiltration in the Napier Complex, east Antarctica. *Earth and Planetary Science Letters*, in press.
- Dallwitz, W.B., 1968. Coexisting sapphirine and quartz in granulites from Enderby Land, Antarctica. *Nature* 219, 476–477.
- DePaolo, D.J., Manton, W.I., Grew, E.S., Halpern, M., 1982. Sm–Nd, Rb–Sr and U–Th–Pb systematics of granulite facies rocks from Fyfe Hills, Enderby Land, Antarctica. *Nature* 298, 614–618.
- Ellis, D.J., 1980. Osumilite–sapphirine–quartz granulites from Enderby Land, Antarctica: P–T conditions of metamorphism, implications for garnet–cordierite equilibria and the evolution of the deep crust. *Contrib. Mineral Petrol.* 74, 201–210.
- Ellis, D.J., Sheraton, J.W., England, R.N., Dallwitz, W.B., 1980. Osumilite–sapphirine–quartz granulites from Enderby Land, Antarctica—mineral assemblages and reactions. *Contrib. Mineral Petrol.* 72, 123–143.
- Grew, E.S., 1980. Sapphirine + quartz association from Archaean rocks in Enderby Land, Antarctica. *Am. Mineralogist* 65, 821–836.
- Grew, E.S., 1982. Osumilite in the sapphirine–quartz terrane of Enderby Land, Antarctica: implications for osumilite petrogenesis in the granulite-facies. *Am. Mineralogist* 67, 762–787.
- Grew, E.S., 1998. Boron and beryllium minerals in granulite-facies pegmatites and implications of beryllium pegmatites for the origin and evolution of the Archaean Napier Complex of East Antarctica. *Memoirs of National Institute of Polar Research, Special Issue*, 53, 74–92.
- Grew, E.S., Manton, W.I., 1979. Archaean rocks in Antarctica: 2.5-billion-year uranium–lead ages of pegmatites in Enderby Land. *Science* 206, 443–445.
- Grew, E.S., Manton, W.I., Sandiford, M., 1982. Geochronological studies in East Antarctica: age of pegmatites in Casey Bay, Enderby Land. *Antarct. J. US* 17, 1–2.
- Harley, S.L., 1985a. Garnet–orthopyroxene bearing granulites from Enderby Land, Antarctica: metamorphic pressure–temperature–time evolution of the Archaean Napier Complex. *J. Petrol.* 26, 819–856.
- Harley, S.L., 1985b. Paragenetic and mineral-chemical relationships in orthoamphibole-bearing gneisses from Enderby Land, east Antarctica: a record of Proterozoic uplift. *J. Metamorphic Geol.* 3, 179–200.
- Harley, S.L., 1987. Pyroxene-bearing granulites from Tonagh Island, Enderby Land, Antarctica: further evidence for very high temperatures (>950 °C) Archaean regional metamorphism in the Napier Complex. *J. Metamorphic Geol.* 5, 241–356.
- Harley, S.L., 1998. An appraisal of peak temperatures and thermal histories in ultra high-temperature (UHT) crustal metamorphism: the significance of aluminous orthopyroxene. *Memoirs of National Institute of Polar Research, Special Issue*, 53, 49–73.
- Harley, S.L., Black, L.P., 1987. The Archaean geological evolution of Enderby Land, Antarctica. In: Park, R.G., Tarney, J. (Eds.), *Evolution of the Lewisian and Comparable Precambrian High-grade Terrains*. Geological Society Special Publication No. 27, pp. 285–296.
- Harley, S.L., Hensen, B.J., 1990. Archaean and Proterozoic high-grade terranes of East Antarctica (40°E–60°E): a case study of the diversity in granulite facies metamorphism. In: Ashworth, J.R., Brown, M. (Eds.), *High Temperature Metamorphism and Crustal Anatexis*. Unwin Hyman, London, pp. 320–370.

- Harley, S.L., Black, L.P., 1997. A revised Archaean chronology for the Napier Complex, Enderby Land, from SHRIMP ion-microprobe studies. *Antarct. Sci.* 9, 74–91.
- Harley, S.L., Motoyoshi, Y., 2000. Al zoning in orthopyroxene in a sapphirine quartzite: evidence for >1120 °C UHT metamorphism in the Napier Complex, Antarctica, and implications for the entropy of sapphirine. *Contrib. Mineral Petrol.* 138, 293–307.
- Hensen, B.J., Motoyoshi, Y., 1992. Osumilite-producing reactions in high temperature granulites from the Napier Complex, East Antarctica: tectonic implications. In: Yoshida, Y., Kaminuma, K., Shirashi, K. (Eds.), *Recent Progress in Antarctica Earth Science*. Terra Scientific Publishing Company, Tokyo, pp. 87–92.
- Kelly, N.M., Clarke, G.L., Carson, C.J., White, R.W., 2000. Thrusting in the lower crust: evidence from the Oygarden Islands, Kemp Land, East Antarctica. *Geol. Mag.* 137, 219–234.
- Lovering, J.F., 1979. The evidence for (4000 m.y. crustal material in Archaean times. *J. Geol. Soc. Aust.* 26, 268 abstract.
- Ludwig, K.R., 1998. On the treatment of concordant uranium-lead ages. *Geochim. Cosmochim. Acta* 62, 315–318.
- Ludwig, K.R., 1999. User's manual for Isoplot/Ex, v2.3, a geochronological toolkit for Microsoft Excel. Berkeley Geochronological Centre Special Publication No. 1a, pp. 54.
- McLaren, A.C., Fitzgerald, J.D., Williams, I.S., 1994. The microstructure of zircon and its influence on the age determination from Pb/U isotopic ratios measured by ion microprobe. *Geochim. Cosmochim. Acta* 58, 993–1005.
- Maas, R., Kinny, P.D., Williams, I.S., Froude, D.O., Compston, W., 1992. The earth's oldest known crust: a geochronological and geochemical study of 3900–4200 Ma old detrital zircons from Mt. Narryer and Jack Hills, Western Australia. *Geochim. Cosmochim. Acta* 56, 1281–1300.
- Miyamoto, T., Grew, E.S., Sheraton, J.W., Yates, M.G., Dunkley, D.J., Carson, C.J., Yoshimura, Y., Motoyoshi, Y., 2000. Lamproite dykes in the Napier Complex at Tonagh Island, Enderby Land, East Antarctica. *Polar Geosci.* 13, 41–59.
- Osanai, Y., Toyoshima, T., Owada, M., Tsunogae, T., Hokada, T., Crowe, W.A., 1999. Geology of Ultrahigh-Temperature metamorphic rocks from Tonagh Island in the Napier Complex, East Antarctica. *Polar Geosci.* 12, 1–28.
- Owada, M., Osanai, Y., Kagami, H., 1994. Isotopic equilibration age of Sm–Nd whole-rock system in the Napier Complex (Tonagh Island), East Antarctica. *Proc. NIPR Symp. Antarct. Geosci.* 7, 122–132.
- Paces, J.B., Miller, J.D., 1993. Precise U–Pb ages of Duluth Complex and related mafic intrusions, Northeastern Minnesota: geochronological insights to physical, petrogenetic, paleomagnetic, and tectonomagnetic processes associated with the 1.1 Ga midcontinental rift system. *J. Geophys. Res.* 98, 13997–14013.
- Quidelleur, X., Grove, M., Lovera, O.M., Harrison, T.M., Yin, A., Ryerson, F.J., 1997. The thermal evolution and slip history of the Renbu Zedong Thrust, southeastern Tibet. *J. Geophys. Res.* 102, 2659–2679.
- Sandiford, M., 1985. The origin of retrograde shear zones in the Napier Complex: implications for the tectonic evolution of Enderby Land, Antarctica. *J. Struct. Geol.* 7, 477–488.
- Sandiford, M., Wilson, C.J.L., 1984. The structural evolution of the Fyfe Hills-Khmara Bay region, Enderby Land, East Antarctica. *Aust. J. Earth Sci.* 31, 403–426.
- Sandiford, M., Powell, R., 1986a. Pyroxene exsolution in granulites from Fyfe Hills, Enderby Land, Antarctica: evidence for 1000 °C metamorphic temperatures in Archaean continental crust. *Am. Mineralogist* 71, 946–954.
- Sandiford, M., Powell, R., 1986b. The origin of Archaean gneisses in the Fyfe Hills region, Enderby Land; field occurrence, petrology and geochemistry. *Precambrian Res.* 31, 37–68.
- Sheraton, J.W., Black, L.P., 1981. Geochemistry and geochronology of Proterozoic tholeiite dykes of East Antarctica: evidence for mantle metasomatism. *Contrib. Mineral Petrol.* 78, 305–317.
- Sheraton, J.W., Black, L.P., 1983. Geochemistry of Precambrian gneisses: relevance for the evolution of the East Antarctic Shield. *Lithos* 16, 273–296.
- Sheraton, J.W., Tingey, R.J., Black, L.P., Offe, L.A., Ellis, D.J., 1987. Geology of Enderby Land and western Kemp Land, Antarctica. Bureau of Mineral Resources, Australia, Bulletin, no. 223, pp. 51.
- Shirashi, K., Ellis, D.J., Fanning, C.M., Hiroi, Y., Kagami, H., Motoyoshi, Y., 1997. Re-examination of the metamorphic and protolith ages of the Rayner Complex, Antarctic: evidence for the Cambrian (Pan-African) regional metamorphic event. In: Ricci, C.A. (Ed.), *The Antarctic Region: Geological Evolution and Processes*. Terra Antarctica Publication, Siena, pp. 79–88.
- Sobotovitch, E.V., Kamenev, Y.N., Komaristyy, A.A., Rudnik, V.A., 1976. The oldest rocks of Antarctic (Enderby Land). *Int. Geol. Rev.* 18, 371–388.
- Tainosho, Y., Kagami, H., Takahashi, Y., Iizumi, S., Osanai, Y., Tsuchiya, N., 1994. Preliminary result for the Sm–Nd whole-rock age of the metamorphic rocks from Mount Pardoe in the Napier Complex, East Antarctica. *Proc. NIPR Symp. Antarct. Geosci.* 7, 115–121.
- Tainosho, Y., Kagami, H., Hamamoto, T., Takahashi, Y., 1994. Preliminary result for the Nd and Sr isotope characteristics of the Archaean gneisses from Mount Pardoe, Napier Complex, East Antarctica. *Proc. NIPR Symp. Antarct. Geosci.* 10, 92–101.
- Wiedenbeck, M., 1995. An example of reverse discordance during ion microprobe zircon dating—an artifact of enhanced ion yields from a radiogenic labile Pb. *Chem. Geol.* 125, 197–218.

Williams, I.S., Compston, W., Black, L.P., Ireland, T.R., Foster, J.J., 1984. Unsupported radiogenic Pb in zircon: a cause of anomalously high Pb–Pb, U–Pb and Th–Pb ages. *Contrib. Mineral Petrol.* 88, 322–327.

Williams, I.S., Claesson, S., 1987. Isotopic evidence for the Precambrian provenance and Caledonian metamorphism of high grade paragneisses from the Seve Nappes, Scandinavian Caledonides. *Contrib. Mineral Petrol.* 97,205–217.